[32] Hattori, Y., Goto, Y., Sakuta, R., Nonaka, I., Mizuna, Y. and Horai, S. (1994) *J. Neurol. Sci.*, **125,** 50-55.

[33] Rayment, I., Holden,H.M., Sellers, J.R., Fananapazir, L. and Epstein, N.D. (1995) *Proc. Natl. Acad. Sci. USA,* **92,** 3864-3868.

[34] Nishi,H., Kimura, A., Harada, H., Toshima, H., Sasazuki, T. (1992) *Biochem. Biophys. Res. Commun.*, **188,** 379-387.

[35] Koyanagi,T. (1996) http://www.angis.org.au/Databases/Heart/heartbreak.html.

[36] Rychlik, W., Spencer, W.J., Rhoads, R.E. (1990) *Nucl. Acids Res,*, **18,** 6409-6412.

[37] Rigler, R., Widengren, J. and Mets, U. (1992) *In Fluorescence Spectroscopy : new methods and applications.* (Wolfbeis, O.S. Ed.), Springer-Verlag, Berlin. pp 12-24.

THE JOURNAL OF BIOLOGICAL CHEMISTRY
Vol. 278, No. 8, Issue of February 21, pp. 6433–6439, 2003
Printed in U.S.A.
© 2003 by The American Society for Biochemistry and Molecular Biology, Inc.

Cell Density and Growth-dependent Down-regulation of Both Intracellular Calcium Responses to Agonist Stimuli and Expression of Smooth-surfaced Endoplasmic Reticulum in MC3T3-E1 Osteoblast-like Cells*

Received for publication, October 7, 2002, and in revised form, December 4, 2002
Published, JBC Papers in Press, December 5, 2002, DOI 10.1074/jbc.M210243200

Toshiyuki Koizumi‡, Hisako Hikiji‡§¶, Wee Soo Shin§, Tsuyoshi Takato‡, Satoru Fukuda‖, Takahiro Abe‡, Noboru Koshikiya‡, Kuniaki Iwasawa§**, and Teruhiko Toyo-oka§****

*From the Departments of ‡Oral and Maxillofacial Surgery, ‖Pathology, and **Organ Pathology and Internal Medicine, Faculty of Medicine, and §Health Service Centre, University of Tokyo, Bunkyo-ku, Tokyo 113-8655, Japan*

A two-dimensional intracellular Ca^{2+} ($[Ca^{2+}]_i$) imaging system was used to examine the relationship between $[Ca^{2+}]_i$ handling and the proliferation of MC3T3-E1 osteoblast-like cells. The resting $[Ca^{2+}]_i$ level in densely cultured cells was 1.5 times higher than the $[Ca^{2+}]_i$ level in sparsely cultured cells or in other cell types (mouse fibroblasts, rat vascular smooth muscle cells, and bovine endothelial cells). A high resting $[Ca^{2+}]_i$ level may be specific for MC3T3-E1 cells. MC3T3-E1 cells were stimulated with ATP (10 μM), caffeine (10 mM), thapsigargin (1 μM), or ionomycin (10 μM), and the effect on the $[Ca^{2+}]_i$ level of MC3T3-E1 cells was studied. The percentage of responding cells and the degree of $[Ca^{2+}]_i$ elevation were high in the sparsely cultured cells and low in densely cultured cells. The rank order for the percentage of responding cells and magnitude of the Ca^{2+} response to the stimuli was ionomycin > thapsigargin = ATP > caffeine and suggests the existence of differences among the various $[Ca^{2+}]_i$ channels. All Ca^{2+} responses in the sparsely cultured MC3T3-E1 cells, unlike in other cell types, disappeared after the cells reached confluence. Heptanol treatment of densely cultured cells restored the Ca^{2+} response, suggesting that cell-cell contact is involved with the confluence-dependent disappearance of the Ca^{2+} response. Immunohistological analysis of type 1 inositol trisphosphate receptors and electron microscopy showed distinct expression of inositol trisphosphate receptor proteins and smooth-surfaced endoplasmic reticulum in sparsely cultured cells but reduced levels in densely cultured cells. These results indicate that the underlying basis of confluence-dependent $[Ca^{2+}]_i$ regulation is down-regulation of smooth-surfaced endoplasmic reticulum by cell-cell contacts.

The calcium ion (Ca^{2+}) acts as an intracellular messenger and regulates a diverse array of functions in many types of cells (1). Various substances that influence bone remodeling modify the intracellular Ca^{2+} ($[Ca^{2+}]_i$) concentration in osteoblasts (2). There are two sources of $[Ca^{2+}]_i$ in osteoblasts: 1) inflow from the extracellular space and 2) release from intracellular stores, such as the endoplasmic reticulum. The release of Ca^{2+} from the endoplasmic reticulum is a ubiquitous signal in many cells including osteoblasts (3, 4). ATP and caffeine cause inositol trisphosphate (IP_3)[1]-induced Ca^{2+} release (IICR) and Ca^{2+}-induced Ca^{2+} release (CICR), respectively, from intracellular Ca^{2+} stores.

We previously reported that the response of the Ca^{2+} level in vascular smooth muscle cells (5) to various stimuli is heterogeneous and that it is dependent on the stage of cell growth (6). A heterogeneous Ca^{2+} response has also been reported in an osteosarcoma cell line stimulated by parathyroid hormone (7) and among sub-cell lines of MC3T3-E1 cells treated with bradykinin (8). In the present study, we examined the effects of cell density and growth on $[Ca^{2+}]_i$-handling mechanisms in MC3T3-E1 cells using a two-dimensional fura-2 imaging system, immunocytochemistry, and electron microscopy, and we identified unique characteristics of these cells. We studied the effect of growth on $[Ca^{2+}]_i$-handling mechanisms in MC3T3-E1 cells by studying the Ca^{2+} dynamics in cells seeded in the sparse or dense condition.

EXPERIMENTAL PROCEDURES

Reagents—All reagents used were of analytical grade. Thapsigargin (TG; Sigma Chemical) and ionomycin (IM; Sigma Chemical) were dissolved in dimethyl sulfoxide (Me_2SO) and then diluted with phosphate-buffered saline (PBS). The final concentration of Me_2SO was less than 0.1% (v/v) and had no action on the handling of $[Ca^{2+}]_i$ in the MC3T3-E1 cells (data not shown). Caffeine and ATP were purchased from Wako Pure Chemicals (Osaka, Japan). Each reagent was administered by replacing half the volume of extracellular medium with medium containing 2-fold concentrated reagent (5, 6). In a pilot study, we attempted to identify suitable reagents and their appropriate concentrations to analyze the transient $[Ca^{2+}]_i$ currents. We used 10 mM caffeine, 10 μM ATP, 1 μM TG, and 10 μM ryanodine or IM in the present study.

Cell Culture—MC3T3-E1 mouse clonal osteogenic cells (a generous gift from Prof. S. Yamamoto, Ohu University, Koriyama, Japan) were seeded onto dishes (radius, 1 cm) made of fluorescence-free glass at a density of 1.0×10^4 cells/dish (sparse condition) or 2.0×10^5 cells/dish (dense condition). The cells were cultured in α-minimal essential medium (Invitrogen) containing 10% fetal bovine serum (Bioserum, Victoria, Australia), 100 units/ml penicillin, 100 μg/ml streptomycin, and 0.25 μg/ml amphotericin B (Sigma Chemical). The medium was

* This study was financially supported by grants-in-aid from the Ministry of Education, Culture, Sports, Science, and Technology and the Ministry of Health, Labor, and Welfare. The costs of publication of this article were defrayed in part by the payment of page charges. This article must therefore be hereby marked "*advertisement*" in accordance with 18 U.S.C. Section 1734 solely to indicate this fact.

¶ To whom correspondence should be addressed: University of Tokyo, 7-3-1, Hongo, Bunkyo-ku 113-8655, Tokyo, Japan. Tel.: 81-3-5800-8669; Fax: 81-3-5800-6832; E-mail: hikiji-ora@h.u-tokyo.ac.jp.

[1] The abbreviations used are: IP_3, inositol trisphosphate; IICR, inositol trisphosphate-induced Ca^{2+} release; CICR, Ca^{2+}-induced Ca^{2+} release; F_{340}/F_{380}, 340- to 380-nm fluorescence ratio; TG, thapsigargin; IM, ionomycin; PBS, phosphate-buffered saline; EC, endothelial cell(s); IP_3-R_1, inositol trisphosphate type-1 receptor; sER, smooth-surfaced endoplasmic reticulum.

changed every 48 h after seeding. Caffeine, ATP, TG, or IM was added between 0 and 120 h after seeding, and the peak $[Ca^{2+}]_i$ level upon stimulation was studied. The resting $[Ca^{2+}]_i$ level in MC3T3-E1 cells seemed to be higher than that in other cells. We compared the $[Ca^{2+}]_i$ level in MC3T3-E1 cells with that in endothelial cells (ECs) from the bovine aorta, cloned rat vascular smooth muscle cells (A_{7r5}), and cloned mouse fibroblasts (NIH3T3), which have been used in studies on $[Ca^{2+}]_i$ dynamics (5, 6). In single-cell line cultures, each cell line was seeded at a density of 1.0×10^4 cells/dish and cultured for 48 h. In cocultures, EC, A_{7r5}, or NIH3T3 cells were seeded together with MC3T3-E1 cells at a density of each cell line of 1.0×10^4 cells/dish and cultured for 48 h.

To examine the effect of cell-cell contact, MC3T3-E1 cells were seeded in dishes at a density of 2.0×10^5 cells/dish (dense condition). After 24 h, 3 μM heptanol, a gap-junctional inhibitor (9, 10), was added to the dishes and the cells were cultured for an additional 48 h. And then, ATP, TG, or IM was added, and the peak $[Ca^{2+}]_i$ level upon stimulation was studied.

Two-dimensional (2D) Image Analysis of $[Ca^{2+}]_i$—The $[Ca^{2+}]_i$ level within individual cells was analyzed as described previously (11–13). Briefly, the cells were washed with PBS and incubated in PBS(+) containing 137 mM NaCl, 2.7 mM KCl, 8.1 mM Na_2HPO_4, 1.5 mM KH_2PO_4, 0.5 mM $MgCl_2$, and 1 mM Ca^{2+}, pH 7.4. The Ca^{2+}-free solution consisted of PBS in which $CaCl_2$ was replaced by 1.0 mM EGTA. Cells were loaded with 4 μM fura-2/acetoxymethyl ester in the same buffer at 37 °C for 30 min, rinsed twice with PBS(+), and then preincubated at 37 °C for an additional 10 min. The recorded fluorescence images were digitized using an on-line image processor (Olympus-Merlin, Tokyo, Japan; Fig. 1*A*). Fig. 1*B* shows the change in the relative value of the 340- to 380-nm fluorescence ratio (F_{340}/F_{380}) in MC3T3-E1 cells upon treatment with ATP. Because of the difficulty in measuring the absolute $[Ca^{2+}]_i$ concentration caused by problems intrinsic to fura-2 fluoroscopy, the maximum amplitude of the $[Ca^{2+}]_i$ elevation in response to each stimulant was expressed as the relative value of F_{340}/F_{380} in relation to the value of F_{340}/F_{380} in the resting state (5, 6).

Caffeine transiently increased the $[Ca^{2+}]_i$ level, in both the presence and the absence of extracellular Ca^{2+} ($[Ca^{2+}]_o$). The degree of $[Ca^{2+}]_i$ elevation evoked by caffeine in the Ca^{2+}-free solution became progressively smaller as the incubation time increased (data not shown). To avoid fluctuations in the response, we applied caffeine to cells in the presence of 1 mM $[Ca^{2+}]_o$. Ryanodine (10 μM; Wako Pure Chemicals) was also added to keep the CICR channels open (14) and to prevent the activation of additional CICR. All measurements were made 24 h after seeding to avoid the effects of trypsin, which was used in seeding, on the Ca^{2+} channels.

Immunohistochemistry—MC3T3-E1 cells incubated in plastic dishes (60 mm in diameter) were fixed with a mixture of equal volumes of ethanol and acetone. The nonspecific binding of antibody was blocked by goat serum, and then the cells were treated with anti-IP_3 type-1 receptor (IP_3-R_1) polyclonal antibody or non-immunized rabbit IgG at room temperature for 1 h, followed by an LSAB2 kit/horseradish peroxidase (DAKO Corporation, Carpinteria, CA). The immunoproduct was visualized by treatment with amino-9-ethylcarbazol (DAKO) and micrographs were taken at 100× (AX-80; Olympus, Tokyo, Japan).

Electron Microscopy—For transmission electron microscopy, the MC3T3-E1 cells were detached from the culture dishes by treatment with trypsin and washed three times with PBS, pH 7.4. After fixing overnight in 2% paraformaldehyde plus 2.5% glutaraldehyde in phosphate buffer, the cells were sedimented at 2000 rpm at room temperature for 5 min, postfixed with 1% osmium tetroxide, dehydrated in graded alcohol, and then embedded in Epon (Epon 812; TAAB Lab, Berkshire, England) overnight at 60 °C. Ultrathin sections (60 nm) were stained with uranyl acetate and lead citrate and observed under an electron microscope (H-7000; Hitachi, Tokyo, Japan).

Statistical Analysis—Data were expressed as the mean ± S.E. and were analyzed by one-way analysis of variance. Treatment pairs were compared by Scheffé's F test. All differences were considered to be statistically significant at $p < 0.05$.

RESULTS

$[Ca^{2+}]_i$ in the Resting State—The $[Ca^{2+}]_i$ level in MC3T3-E1 cells in the resting state that had been seeded in the sparse or dense condition was measured at 0, 24, 48, 72, and 120 h after the first medium change (Fig. 2). The $[Ca^{2+}]_i$ level of the densely seeded cells was 1.5 times higher than that of the sparsely seeded cells at 0 h (1.19 ± 0.01 *versus* 0.80 ± 0.02, $p < 0.01$). The $[Ca^{2+}]_i$ level of the densely seeded cells increased slightly, although significantly, up through 120 h from 1.19 ± 0.01 to 1.33 ± 0.01 ($p < 0.01$). The $[Ca^{2+}]_i$ level of the sparsely seeded cells increased significantly from 0.80 ± 0.02 to 1.30 ± 0.01 at 120 h ($p < 0.01$) and reached the same level as that of the densely seeded cells at 120 h (1.33 ± 0.01, densely seeded, *versus* 1.30 ± 0.01, sparsely seeded), with no significant change thereafter. These results indicate that the $[Ca^{2+}]_i$ level of MC3T3-E1 cells increased as proliferation progressed.

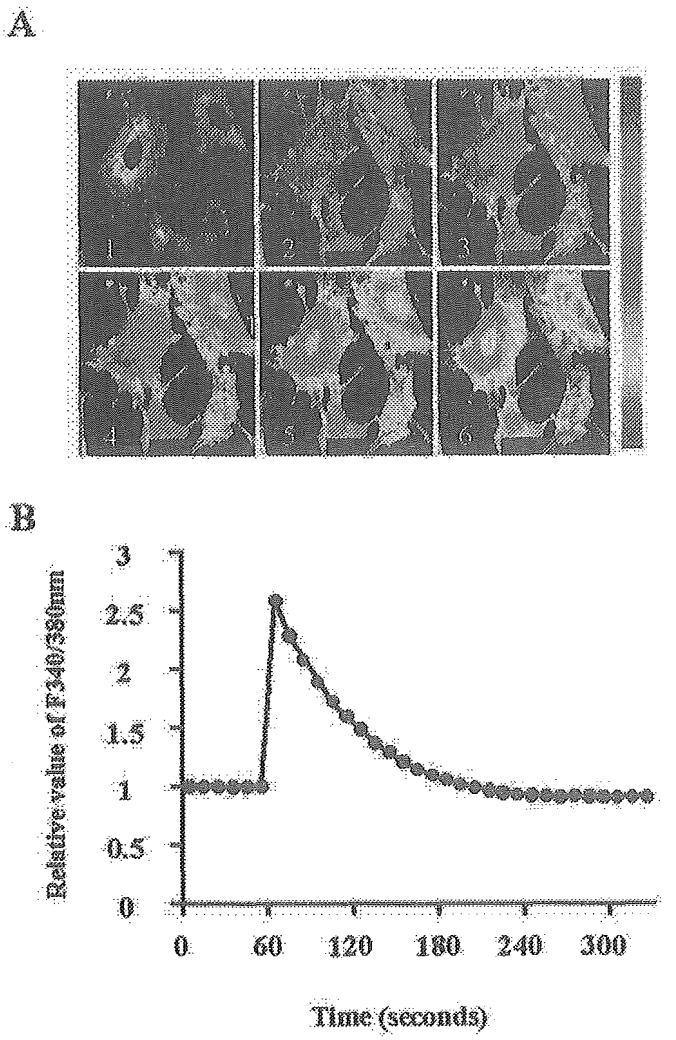

FIG. 1. **Two-dimensional images of the Ca^{2+} response (*A*) and Ca^{2+} dynamics (*B*) in MC3T3-E1 cells induced by ATP (10 μM).** ATP was applied at 60 s. *A*, *1–6*. $[Ca^{2+}]_i$ response at 0, 70, 85, 95, 105, and 115 s, respectively, after ATP stimulation. *B*, the relative level of $[Ca^{2+}]_i$ is shown (expressed as the relative value of F_{340}/F_{380} compared with the F_{340}/F_{380} in the resting state) at various time points after ATP was applied.

To confirm that densely seeded MC3T3-E1 cells in the resting state have a high $[Ca^{2+}]_i$ level, we measured the $[Ca^{2+}]_i$ level in both isocultures and cocultures with other cell lines, including mouse fibroblasts (NIH3T3), rat vascular smooth muscle cells (A_{7r5}), and ECs from the bovine aorta. The resting state $[Ca^{2+}]_i$ level of MC3T3-E1 cells was higher than that of the other cell lines both in the isocultures, in which one cell line each had been harvested (Fig. 3*A*), and in the cocultures at 48 h, in which two cell lines had been cultured in the same dish (Fig. 3*B*). These results suggest that the high $[Ca^{2+}]_i$ level in resting state MC3T3-E1 cells may exert a specific function in calcifying tissue.

Effects of ATP and Caffeine on $[Ca^{2+}]_i$ Release from Intracellular Ca^{2+} Stores at Different Cell Densities during Cell Proliferation—In the following experiments, MC3T3-E1 cells were

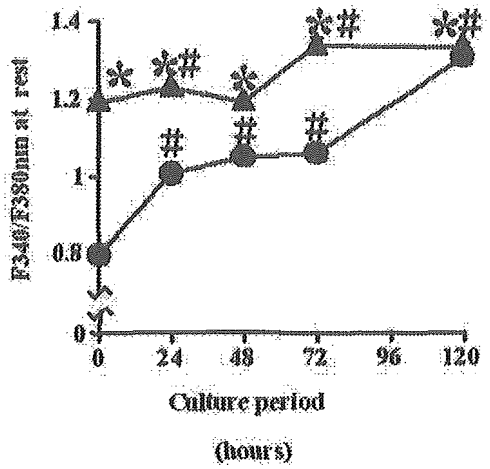

FIG. 2. **Relationship between the resting $[Ca^{2+}]_i$ level in MC3T3-E1 cells and length of the culture period.** The $[Ca^{2+}]_i$ level of densely seeded cells (▲) was 1.5 times higher than that of sparsely seeded cells (●) at 0 h. Each *point* represents the mean ± S.E. of 60 responder cells in three cultures. *, $p < 0.05$, significant difference between sparsely and densely seeded MC3T3-E1 cells. #, significant difference compared with 0 h.

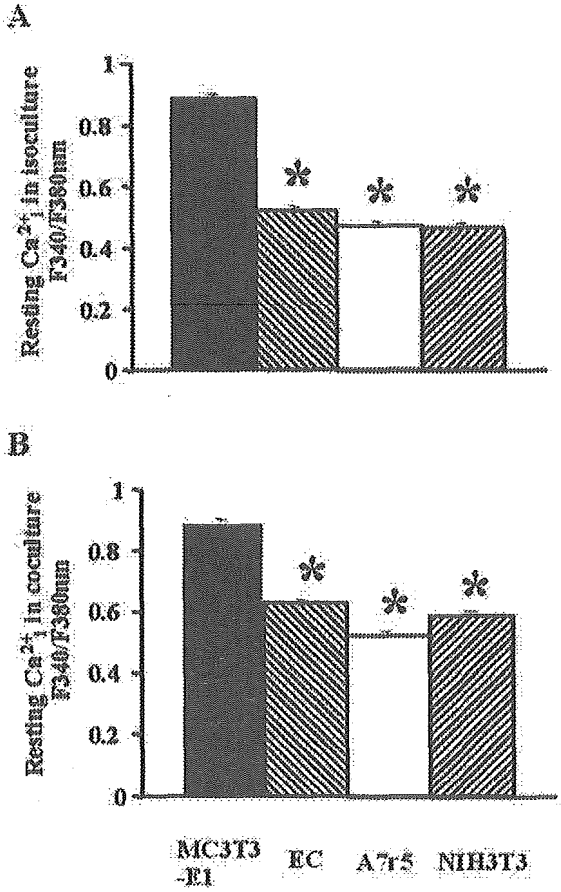

FIG. 3. **Comparison of the resting state $[Ca^{2+}]_i$ level among MC3T3-E1, EC, A_{7r5}, and NIH3T3 cells.** The resting state Ca^{2+} level of MC3T3-E1 cells was higher than that of the other cells both in isoculture (*A*) and coculture (*B*). *, $p < 0.05$, significant difference compared with that in MC3T3-E1 cells. Each *bar* represents the mean ± S.E. of three cultures.

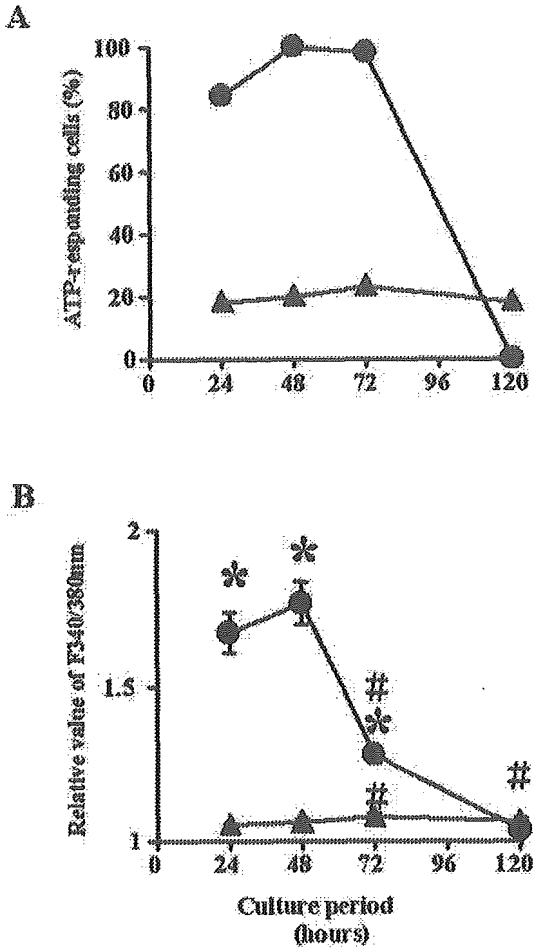

FIG. 4. **Effect of ATP on the $[Ca^{2+}]_i$ level in MC3T3-E1 cells.** *A*, percentage of ATP-responding cells under sparsely (●) and densely (▲) seeded conditions during cell proliferation. *B*, relative value of F_{340}/F_{380} upon ATP stimulation in responder cells under sparse (●) and dense (▲) conditions. Each *point* represents the mean ± S.E. of 60 responder cells in three cultures. *, $p < 0.05$, significant difference between MC3T3-E1 cells seeded in sparse and dense conditions. #, significant difference compared with that at 24 h.

incubated in PBS in which $CaCl_2$ had been replaced with EGTA (1.0 mM) to prevent Ca^{2+} influx into cells and to selectively evaluate Ca^{2+} release from intracellular calcium stores. ATP (10 μM), which stimulates IICR (15, 16), elevated the $[Ca^{2+}]_i$ level in 84% of the sparsely seeded cells when it was applied at 24 h after seeding, in 100% of the cells when applied at 48 h, and in 98% of the cells when applied at 72 h (Fig. 4*A*). In contrast, ATP elevated the $[Ca^{2+}]_i$ level in only 18–23% of the densely seeded cells when it was applied between 24 and 120 h. The relative value of F_{340}/F_{380} upon treatment with ATP at 24 and 48 h in each responder cell in the culture under the sparsely seeded condition was 1.675 ± 0.066 and 1.770 ± 0.068, respectively. Then, it sharply decreased to 1.279 ± 0.023 and 1.038 ± 0.003 when ATP was applied at 72 and 120 h, respectively, when the cell density, because of proliferation, reached that of the densely seeded cells (Fig. 4*B*).

Caffeine, which stimulates CICR (14), increased the $[Ca^{2+}]_i$ level in 61 and 79% of the sparsely seeded cells when it was applied at 24 and 48 h after seeding, respectively. When caffeine was applied at 72 or 120 h, only 0–3% of the sparsely seeded cells had an increased $[Ca^{2+}]_i$ level (Fig. 5*A*). In the densely seeded cells, caffeine had no effect on the $[Ca^{2+}]_i$ level when it was applied between 24 and 120 h after seeding. In sparsely seeded cells, the relative value of F_{340}/F_{380} was 1.115 ± 0.009 when caffeine was applied at 24 h, and it increased to 1.199 ± 0.028 when applied at 48 h (Fig. 5*B*). These results indicate that caffeine affected the $[Ca^{2+}]_i$ level in MC3T3-E1 cells more heterogeneously than ATP and that the degree of heterogeneity upon treatment with caffeine or ATP was affected by the cell density.

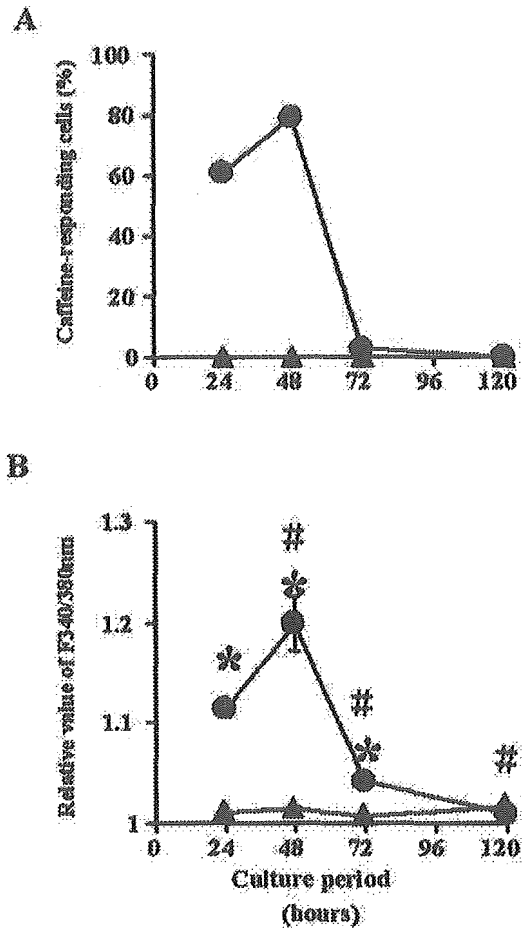

FIG. 5. **Effect of caffeine on the $[Ca^{2+}]_i$ level in MC3T3-E1 cells.** *A*, percentage of caffeine-responding cells under sparsely (●) and densely (▲) seeded conditions during cell proliferation. *B*, relative value of F_{340}/F_{380} upon treatment with caffeine in the sparsely (●) and densely (▲) seeded conditions. Each *point* represents the mean ± S.E. of 60 responder cells in three cultures. *, $p < 0.05$, significant difference between MC3T3-E1 cells seeded in sparse and dense conditions. #, significant difference compared with that at 24 h.

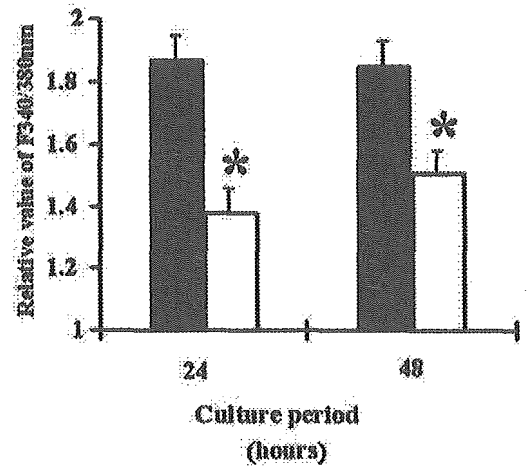

FIG. 6. **Comparison of the relative value of F_{340}/F_{380} upon treatment with ATP between caffeine-responded (*black columns*) and non-responded (*white columns*) MC3T3-E1 cells at 24 or 48 h in the sparse condition.** Each *bar* represents the mean ± S.E. of three cultures. *, $p < 0.05$, significant difference between caffeine responded cells and caffeine non-responded cells.

In the sparsely seeded condition, the relative value of F_{340}/F_{380} upon treatment with ATP in caffeine responding cell was larger than that upon treatment with ATP in caffeine non-responding cell at 24 and 48 h (Fig. 6). These results indicate that cells that responded to caffeine also responded to ATP and suggest that the source of $[Ca^{2+}]_i$ release was the same smooth-surfaced endoplasmic reticulum (sER) via CICR or IICR, a finding that differs from that in vascular smooth muscle cells under the sparsely seeded condition (5, 6).

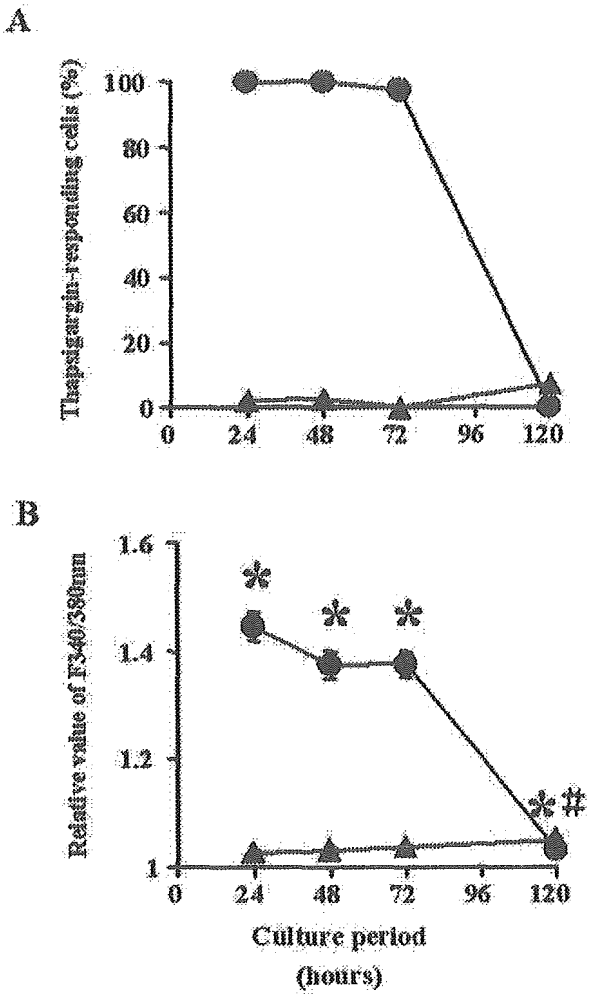

FIG. 7. **Effect of thapsigargin on the $[Ca^{2+}]_i$ level in MC3T3-E1 cells.** *A*, percentage of thapsigargin-responding cells under the sparsely (●) and densely (▲) seeded conditions during cell proliferation. *B*, relative value of F_{340}/F_{380} in responder cells upon treatment with thapsigargin among sparsely seeded cells (●) at 24, 48, or 72 h is high. The F_{340}/F_{380} did not change in the densely seeded cells upon treatment with thapsigargin between 24 and 120 h (▲). Each *point* represents the mean ± S.E. of 60 responder cells in three cultures. *, $p < 0.05$, significant difference between MC3T3-E1 cells seeded in the sparse and dense conditions. #, significant difference compared with that at 24 h.

Effects of Thapsigargin (TG) and Ionomycin (IM) on the $[Ca^{2+}]_i$ Level at Different Cell Densities—TG blocks the uptake of Ca^{2+} from the cytoplasm to the sER (17). When TG was applied at 24, 48, or 72 h, the $[Ca^{2+}]_i$ level increased in 97.5–100% of the sparsely seeded cells; however, upon application of TG at 120 h, none of the cells had an increased $[Ca^{2+}]_i$ level (Fig. 7*A*). The percentage of densely seeded cells with elevated $[Ca^{2+}]_i$ was only 3–8% when TG was applied between 24 and 120 h after seeding. In sparsely seeded cells, the relative value of F_{340}/F_{380} in the responders was 1.445 ± 0.026, 1.375 ± 0.025, and 1.376 ± 0.023 when TG was applied at 24, 48, and 72 h, respectively (Fig. 7*B*). However, the relative value of F_{340}/F_{380} in sparsely seeded cells upon treatment with TG at 120 h and the relative values of F_{340}/F_{380} in densely seeded cells that had been treated with TG at 24, 48, 72, or 120 h did not significantly differ.

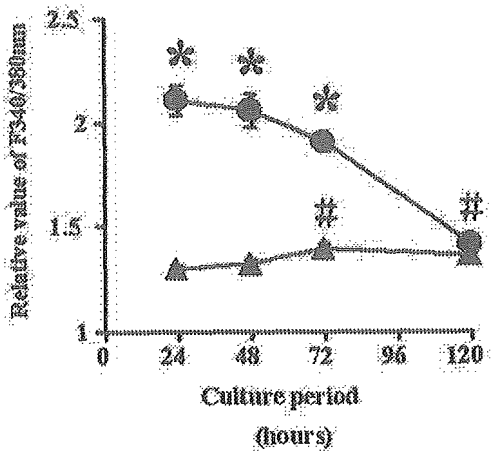

FIG. 8. **Relative value of F_{340}/F_{380} upon treatment with ionomycin in responder cells under sparse (●) and dense (▲) conditions.** Each *point* represents the mean ± S.E. of 60 responder cells in three cultures. *, $p < 0.05$, significant difference between MC3T3-E1 cells seeded in sparse and dense conditions. #, significant difference compared with that at 24 h.

All Ca^{2+} ions in internal stores can be non-specifically released by the Ca^{2+} ionophore, IM (2). IM elevated the $[Ca^{2+}]_i$ level in 100% of the sparsely and densely seeded cells. In the sparsely seeded cells, the relative value of F_{340}/F_{380} upon treatment with IM at 24, 48, 72, or 120 h after seeding was 2.110 ± 0.067, 2.058 ± 0.078, 1.910 ± 0.042, and 1.421 ± 0.021, respectively (Fig. 8). When densely seeded cells were treated with IM, the $[Ca^{2+}]_i$ level increased by a smaller degree. All data on the Ca^{2+} dynamics in the TG and IM experiments supported the dependence of the $[Ca^{2+}]_i$ response on cell density. Furthermore, the Ca^{2+} response was smaller upon treatment with TG than upon treatment with IM at each time point. This may indicate that Ca^{2+} was released from other internal stores in addition to the sER.

Effect of Heptanol on the $[Ca^{2+}]_i$ Response—The relative value of F_{340}/F_{380} upon treatment with ATP, caffeine, TG, or IM in the responders was much lower throughout the experiment in the densely seeded cells than in the sparsely seeded cells (Figs. 4, 5, 7, 8). Heptanol, a gap-junctional inhibitor (9, 10), was used to evaluate the effect of cell-cell contact in the densely seeded cells. When densely seeded cells were treated with 3 μM heptanol, the $[Ca^{2+}]_i$ elevation and the relative value of F_{340}/F_{380} upon treatment with ATP, TG, or IM recovered (Fig. 9). These results suggest that cell-cell contact may inhibit the Ca^{2+} response of densely seeded cells to ATP, caffeine, TG, and IM.

Immunodetection of IP_3-R_1—Ca^{2+} was released from CICR channels in response to caffeine only in sparsely seeded cells up to between 48 and 72 h. The Ca^{2+} efflux from IICR channels was also closely related to the Ca^{2+} released from the sER. These results suggest that IICR may play a more significant role than CICR in calcium handling in osteoblasts. To date, three isoforms of the IP_3 receptor have been cloned, and the type-1 receptor is believed to be ubiquitous. Using a specific antibody to IP_3-R_1, we investigated the expression of this receptor in sparsely and densely seeded cells to determine whether it is involved in the Ca^{2+} response. A high level of IP_3-R_1 protein was detected in sparsely seeded cells upon culture for 24 h (Fig. 10*B*), and a low level was detected upon culture for 120 h (Fig. 10*C*). The level of immunostaining was low in densely seeded cells at both 24 and 120 h (Fig. 10, *D* and *E*). The level of IP_3-R_1 protein expression was associated with the amount of Ca^{2+} released from IICR channels.

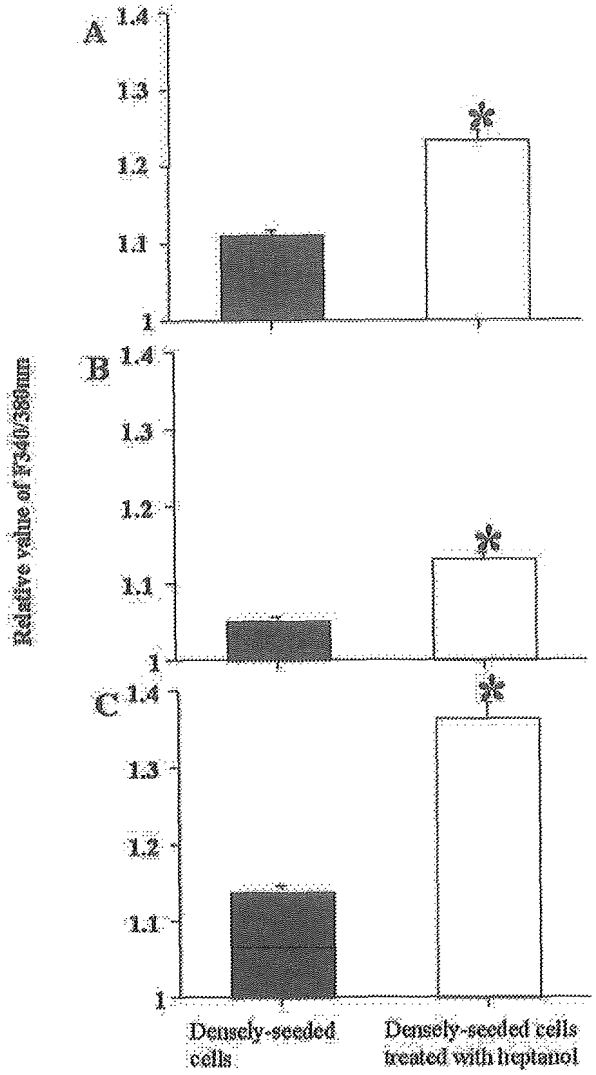

FIG. 9. **Effect of heptanol on the increase in F_{340}/F_{380} induced by ATP (*A*), thapsigargin (*B*), and ionomycin (*C*).** Each *bar* represents the mean ± S.E. of 40 responder cells in two cultures. *, $p < 0.05$, significant difference between densely seeded control cells (*black bars*) and 3 μM heptanol-treated cells (*white bars*).

Electron Microscopy of sER—Transmission electron microscopy was used to ascertain the relationship between the $[Ca^{2+}]_i$ level and the amount of sER in osteoblasts. Many organelles, including sER, were observed in the sparsely seeded cells at 24 h (Fig. 11, *A* and *B*). However, at 120 h of culture, the sER had been reduced, and many rough-surfaced endoplasmic reticula and mitochondria were detected after cell proliferation (Fig. 11, *C* and *D*). Many rough-surfaced endoplasmic reticula and mitochondria were observed and reduced number of sER were seen in densely seeded cells that had been cultured for 24 (Fig. 11, *E* and *F*) or 120 h (Fig. 11, *G* and *H*). Thus, the reduced Ca^{2+} response of densely seeded cells to ATP, caffeine, TG, and IM can be explained by the reduced number of sER. These results suggest that the expression of sER is regulated by cell proliferation.

DISCUSSION

Heterogeneity of the $[Ca^{2+}]_i$ level among MC3T3-E1 cells was observed even before stimulation and was dependent on cell density (sparsely seeded or densely seeded). The $[Ca^{2+}]_i$ level in cells in the resting state ranges from 50 to 400 nM and varies according to cell type and function (14). Because estimation of the absolute $[Ca^{2+}]_i$ level by fura-2 fluorescence is inac-

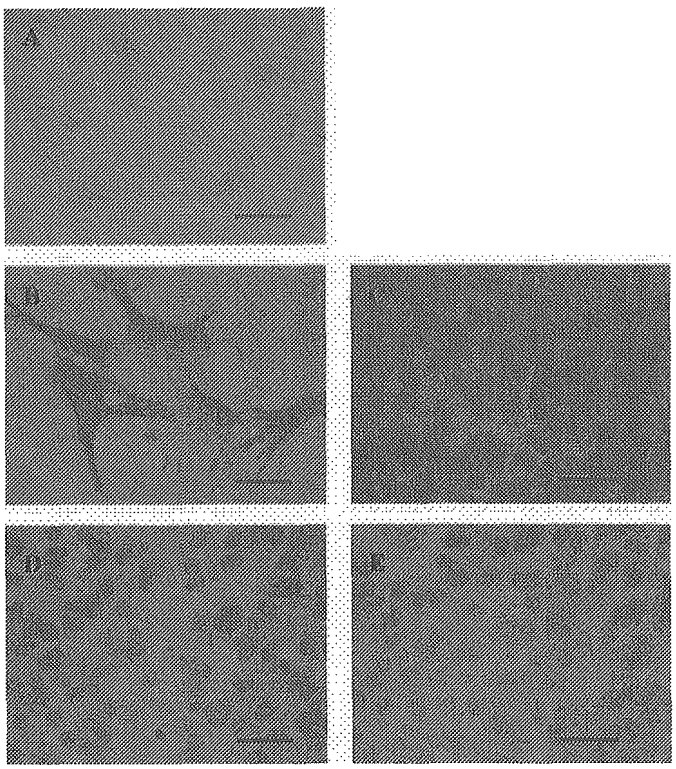

FIG. 10. **Immunodetection of IP_3-R_1.** *A*, negative control in sparsely seeded cells at 24 h. *B*, a high level of IP_3-R_1 was detected in sparsely seeded cells at 24 h. *C*, the level of IP_3-R_1 in sparsely seeded cells decreased at 120 h. The level of staining was weak in densely seeded cells both at 24 (*D*) and 120 h (*E*). Bar, 60 μm.

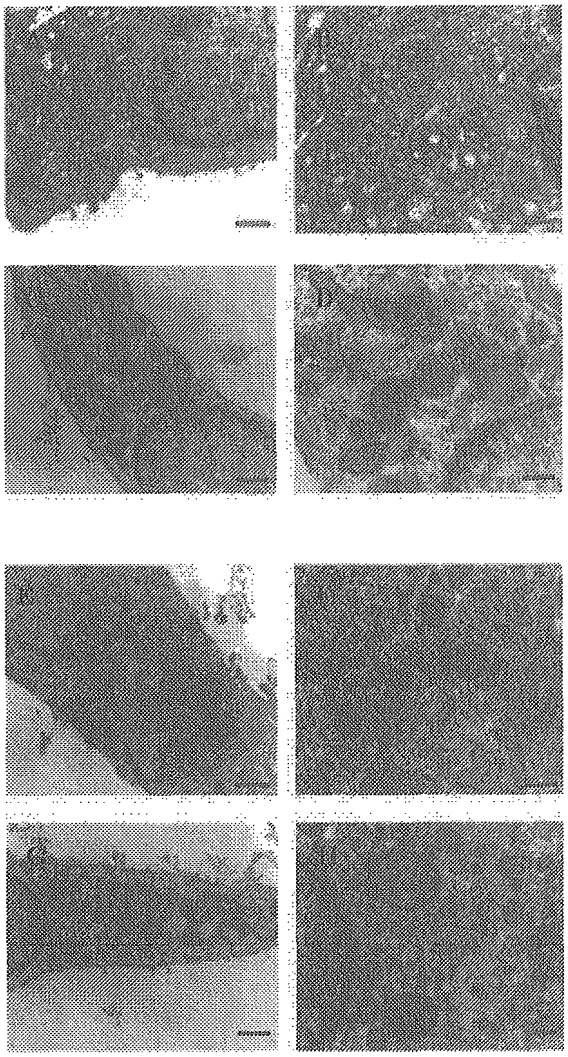

FIG. 11. **Electron microscopic observation of sER.** Many organelles, including sER, are observed in sparsely seeded cells at 24 h (*A* and *B*). However, the sER disappeared and many rough-surfaced endoplasmic reticula and mitochondria are observed at 120 h (*E* and *F*), when the cell density became similar to that of densely seeded cells after cell proliferation. In densely seeded cells, many rough-surfaced endoplasmic reticula and mitochondria are observed and no sER are seen at 24 (*C* and *D*) and 120 h (*G* and *H*). *Bar* in *A*, *C*, *E*, and *G*, 0.5 μm; in *B*, *D*, *F*, and *H*, 0.2 μm.

curate because of several problems intrinsic to fura-2 fluorescence (11–13), the $[Ca^{2+}]_i$ level in the resting state obtained in previous reports cannot be simply compared with that obtained in the present study. The relative value of F_{340}/F_{380} in reference to F_{340}/F_{380} in the resting state (11) was used to evaluate the Ca^{2+} response. To compare the $[Ca^{2+}]_i$ levels of various cells at the resting state, we used F_{340}/F_{380} in iso- and cocultures of MC3T3-E1 cells and other established cell lines (EC, A_{7r5}, and NIH3T3).

It is unclear why the $[Ca^{2+}]_i$ level was higher in the densely seeded MC3T3-E1 cells than in the sparsely seeded cells or other cell lines. We consider that this characteristic is specific for bone-forming MC3T3-E1 osteoblast-like cells. In the densely seeded MC3T3-E1 cells, the number of sER was reduced, indicating a reduced amount of stored Ca^{2+}. Consequently, it is suggested that in the resting state, the $[Ca^{2+}]_i$ level increases. However, the $[Ca^{2+}]_i$ level in densely seeded cells was about 1.5 times higher than that in the sparse condition or other cell lines, and the degree of the increase in $[Ca^{2+}]_i$ level was not necessarily so high that it would be toxic for cells. The presence of an increased $[Ca^{2+}]_i$ level in the resting state of MC3T3-E1 cells, especially in densely seeded cells, seems to be informative for estimating the physiological significance of bone-forming cells. We believe that the increased $[Ca^{2+}]_i$ level may be advantageous for the release of Ca^{2+} during calcification from the point of view of ionic strength.

We focused on the cell density- and growth-dependent changes in the $[Ca^{2+}]_i$ response of osteoblast-like cells to various stimuli. There is a study that focused on the downstream signaling mechanism via Ca^{2+}, not only from internal stores but also from extracellular Ca^{2+} in osteoblasts (18). Whether the $[Ca^{2+}]_i$ response of osteoblast-like cells to various stimuli creates cross-talk with extracellular Ca^{2+}-sensing pathways is of much interest and requires further investigation (19). Among the agonists employed in the present study, ATP, which stimulates IICR, caused $[Ca^{2+}]_i$ elevation when applied between 24 and 120 h to both sparsely and densely seeded cells. In contrast, caffeine, which opens CICR channels, induced $[Ca^{2+}]_i$ elevation in only the sparsely seeded condition. CICR may be inhibited more strongly than IICR in densely seeded cells. On the other hand, cells showing CICR channel function reacted to ATP, and the other cells that did not reveal an IICR channel response did not respond to caffeine either. Therefore, IICR channels mainly handle the calcium response in MC3T3-E1 cells. We previously showed that the expression of CICR and IICR channels, in addition to voltage-dependent Ca^{2+} channels, is influenced by cell growth and enhanced by the differentiation of vascular smooth muscle cells and that they are independently regulated from each other (5, 6). The percentage of responding cells and the magnitude of the Ca^{2+} response were much lower in sparsely seeded vascular smooth muscle cells than in densely seeded cells. Thus, $[Ca^{2+}]_i$ handling in MC3T3-E1 cells differs from that in vascular smooth muscle cells.

TG depletes Ca^{2+} from the sER and induces $[Ca^{2+}]_i$ elevation via capacitative Ca^{2+} entry. A sufficient dose of IM, an ionophore that forms artificial $[Ca^{2+}]_i$ channels in membranes and releases all Ca^{2+} from the sER, also increased the $[Ca^{2+}]_i$ level even when Ca^{2+} entry did not occur in PBS(−). The rank order of the degree of $[Ca^{2+}]_i$ increase was IM > TG = ATP > caffeine. These results indicate that there is a large amount of Ca^{2+} in the sER of sparsely seeded MC3T3-E1 cells and that IICR channels of the sER mainly control $[Ca^{2+}]_i$ elevation in MC3T3-E1 cells. These findings are fundamentally compatible with the results of the study of Zach *et al.* (19). In sparsely seeded MC3T3-E1 cells, the presence of a high level of IP_3-R_1 and a large number of sER was morphologically confirmed by immunohistology and electron microscopy, respectively.

The $[Ca^{2+}]_i$ level in osteoblasts has been reported to be correlated with the seeded cell density, the cell line, morphology, and receptor distribution (7, 8, 12). Various factors influence the $[Ca^{2+}]_i$ level in individual cells at rest and after agonist administration. A previous study suggested that gap junctions and gap-junctional intercellular communication play pivotal mechanotransduction mechanisms in bone (20). In this study, the results of heptanol treatment revealed that gap-junctional cell-cell contact also contributes to the cell density-dependent, heterogeneous $[Ca^{2+}]_i$ response to agonists. In the proliferating phase of osteoblasts, cells without cell-cell contact have both CICR and IICR channels or abundant sER. We previously showed that IP_3-R_1 may regulate the proliferation of vascular smooth muscle cells (21). During bone formation in physiological growth or pathological repair after a bone fracture, enhanced IP_3-R_1 expression may be required for the proliferation of osteoblasts. To elucidate the precise significance of IICR modulation, more specific and detailed studies should be conducted in the future.

REFERENCES

1. Putney, J. W. (1993) *Science* **29,** 676–678
2. Meszaros, J. G., and Karin, H. J. (1995) *J. Bone Miner. Res.* **10,** 704–710
3. Ljunggren, O., Johansson, H., Ljunghall, S., Fredholm, B. B., and Lerner, U. H. (1991) *J. Bone Miner. Res.* **6,** 443–452
4. Kumagai, H., Sacktor, B., and Filburn, C. R. (1991) *J. Bone Miner. Res.* **6,** 697–707
5. Shin, W. S., Toyo-oka, T., Masuo, M., Okai, Y., Fujita, H., and Sugimoto, T. (1991) *Circ. Res.* **69,** 551–556
6. Masuo, M., Toyo-oka, T., Shin, W. S., and Sugimoto, T. (1991) *Circ. Res.* **69,** 1327–1339
7. Wiltink, A., van den Brink, A. M., Herrmann-Erlee, M. P., van der Meer, J. M., van der Plas, A., Willems, P. H., Van Duijn, B., Nijweide, P. J., Ypey, D. L. (1993) *Cell Calcium* **14,** 591–600
8. Leis, H. J., Hulla, W., Gruber, R., Huber, E., Zach, D., Gleispach, H., and Windischhofer, W. (1997) *J. Bone Miner. Res.* **12,** 541–551
9. Ilvesaro, J., Vaananen, K., and Tuukkanen, J. (2000) *J. Bone Miner. Res.* **15,** 919–926
10. Jorgensen, N. R., Geist, S. T., Civitelli, R., and Steinberg, T. H. (1997) *J. Cell Biol.* **139,** 497–506
11. Shin, W. S., Sasaki, T., Kato, M., Hara, K., Seko, A., Yang, W. D., Shimamoto, N., Sugimoto, T., and Toyo-oka, T. (1992) *J. Biol. Chem.* **267,** 20377–20382
12. Civitelli, R., Fujimori, A., Bernier, S. M., Warlow, P. M., Goltzman, D., and Hruska, K. A. (1992) *Endocrinology* **130,** 2392–2400
13. Chen, J., Wang, Y. P., Wang, Y., Nakajima, T., Iwasawa, K., Hikiji, H., Sunamoto, M., Choi, D., Yoshida, Y., Sakaki, Y., Toyo-Oka, T. (2000) *J. Biol. Chem.* **275,** 28739–28749
14. Iino, M., Kobayashi, T., Endo, M. (1988) *Biochem. Biophys. Res. Comm.* **152,** 417–422
15. Shimegi, S. (1996) *Calcif. Tissue Int.* **58,** 109–113
16. Kumagai, H., Sakamoto, H., Guggino, S., Filburn, C. R., Sacktor, B. (1989) *Calcif. Tissue Int.* **45,** 251–254
17. Thastrup, O., Cullen, P. J., Drobak, B. K., Hanley, M. R., Dawson, A. P. (1990) *Proc. Natl. Acad. Sci. U. S. A.* **87,** 2466–2470
18. Goldwin, S. L., and Soltoff, S. P. (2002) *Bone* **30,** 559–566
19. Zach, D., Windischhofer, W., and Leis, H. J. (2001) *Bone* **28,** 595–602
20. Saunders, M. M., You, J., Trosko, J. E., Yamasaki, H., Li, Z., Donahue, H. J., and Jacobs, C. R. (2001) *Am. J. Physiol.* **281,** C1917–C1925
21. Wang, Y., Chen, J., Wang, Y., Taylor, C. W., Hirata, Y., Hagiwara, H., Mkoshiba, K., Toyo-oka, T., Omata, M., Sakai, Y. (2001) *Circ. Res.* **88,** 202–209

Inhibition of Hydroxymethylglutaryl-Coenzyme A Reductase Reduces Th1 Development and Promotes Th2 Development

Rie Hakamada-Taguchi, Yoshio Uehara, Kagemasa Kuribayashi, Atsushi Numabe, Kanako Saito, Hideyuki Negoro, Toshiro Fujita, Teruhiko Toyo-oka, Takuma Kato

Abstract—Several prospective clinical studies have indicated that hydroxymethylglutaryl-coenzyme A reductase inhibitors, statins, prevent cardiovascular events in part through their antiinflammatory properties. Because inflammation is positively and negatively regulated by T helper (Th) 1 cells and Th2 cells, respectively, we examined the effects of statins on the Th polarization in vitro and in vivo. Here we demonstrated that the statins tested, ie, cerivastatin, simvastatin, lovastatin, and atorvastatin, promoted Th2 polarization through both inhibition of Th1 development and augmentation of Th2 development of $CD4^+$ T cells primed in vitro with anti-CD3 antibody and splenic antigen-presenting cells. Cerivastatin exerted most potent effect on modulation of Th1/Th2 development, and the effect was completely abrogated by an addition of mevalonate. Consistent with in vitro experiments, cerivastatin treatment decreased IFN-γ production of lymph node cells from mice immunized with ovalbumin emulsified in complete Freund's adjuvant, indicating that Th1 development is also suppressed in an in vivo proinflammatory environment. In this murine model, cerivastatin significantly reduced mesangial matrix expansion of glomeruli in the kidney and attenuated proteinuria. The decrease of glomerular sclerosis by cerivastatin treatment was positively related to the suppression of interferon (IFN)-γ–producing Th1 response in draining lymph node cells. Hence, these findings strongly suggest that statins' inhibition of 3-hydroxy-3-methylglutaryl-coenzyme A reductase regulates Th1/Th2 polarization in vivo and such a mechanism possibly plays a pathophysiological role in immune-related glomerular injury. **(*Circ Res.* 2003;93: 948-956.)**

Key Words: statins ■ 3-hydroxy-3-methylglutaryl-coenzyme A reductase inhibitors ■ Th1/Th2 ■ inflammation ■ glomerular sclerosis

Naive $CD4^+$ T cells that encounter antigen on antigen-presenting cells (APCs) develop into at least two distinct T helper (Th) cells, ie, Th1 cells secreting interleukin (IL)-2, interferon (IFN)-γ, and tumor necrosis factor-β and Th2 cells secreting IL-4, IL-5, and IL-10. The type of Th cells developed determines outcome of immune responses. Th1 cells mediate proinflammatory cellular immunity, whereas Th2 cells mediate humoral immunity and downregulate inflammatory responses. The development of naive $CD4^+$ T cells into either Th1 or Th2 cells is influenced by several factors, including type of APC, costimulatory molecules, strength of signal delivered to T cell receptor (TCR), and cytokine milieu at early stage of naive $CD4^+$ T cell activation.[1,2] The process of Th development is tightly regulated to evoke appropriate immune responses. With the system unregulated, Th1 and Th2 cells mediate tissue-damaging inflammatory or allergic diseases, respectively.[3]

Statins, inhibitors of 3-hydroxy-3-methylglutaryl-coenzyme A (HMG-CoA) reductase, are potent inhibitors of cholesterol biosynthesis and have greatly improved the management of hypercholesteremia. Several large clinical trials have demonstrated that statins significantly decreased cardiovascular mortality and morbidity over the years.[4,5] However, recent clinical and experimental studies have suggested that some benefits of statins in cardiovascular diseases may be attributed to mechanisms beyond the lipid-lowering effects, including antiinflammatory properties.[5,6] Indeed, in some studies, statins have been shown to reduce serum concentration of C-reactive protein, a marker of inflammation, providing evidence for antiinflammatory effects of statins.[5,7] Concerning the underlying mechanisms, statins inhibit IFN-γ-inducible major histocompatibility complex (MHC) class II expression on macrophages[8] and block lymphocyte function–associated antigen-1 (LFA-1)–dependent stimulation of T cells,[9] both of which might result in suppression of activation of proinflammatory Th1 cells. In addition, recent studies have demonstrated that treatment with atorvastatin prevents and

Original received September 19, 2002; resubmission received August 5, 2003; revised resubmission received October 2, 2003; accepted October 2, 2003.

From the Health Service Center (R.H.-T., Y.U., H.N., T.T.) and Department of Medicine (Y.U., H.N., T.F., T.T.), University of Tokyo, Tokyo, Japan; Department of Bioregulation (K.K., K.S., T.K.), Mie University School of Medicine, Mie, Japan; and Department of Clinical Laboratory Medicine and Institute of Medical Science (A.N.), Dokkyo University School of Medicine, Tochigi, Japan.

Correspondence to Takuma Kato, PhD, Department of Bioregulation, Mie University School of Medicine, 2-174 Edobashi, Tsu-shi, Mie, 514-8507, Japan. E-mail katotaku@doc.medic.mie-u.ac.jp

© 2003 American Heart Association, Inc.

Circulation Research is available at http://www.circresaha.org

DOI: 10.1161/01.RES.0000101298.76864.14

reverses experimental autoimmune encephalomyelitis via suppression and augmentation of Th1 and Th2 immune responses, respectively.[10,11] Simvastatin has been also reported to exhibit therapeutic potential in murine model of rheumatoid arthritis through inhibition of Th1 response.[12] These studies have suggested that beneficial effects of statins on autoimmune diseases were attributable to suppression of Th1 response.

Therefore, to explore the effect of statins on Th1/Th2 development directly, we assayed type of Th cells generated from naive $CD4^+$ T cells in vitro in the presence of several forms of statins. Furthermore, using mice inoculated with antigen in complete Freund's adjuvant (CFA), we investigated the effects of the statins on the Th1/Th2 balance and assessed whether such changes are associated with regression of the kidney injury seen in the immunized mice.

Materials and Methods

Mice

Female C57BL/6 and BALB/c mice were purchased from Japan SLC (Shizuoka, Japan) and used at the age of 6 to 9 weeks. Mice were cared for in accordance with the *Guide for the Care and Use of Laboratory Animals* (revised 1996, National Academy Press, Washington, DC). All experiments were approved by our institutional ethical committee for animal welfare.

Culture Media

RPMI1640 (Sigma), supplemented with 10% FBS (CSL Ltd), 5×10^{-5} mol/L 2-mercaptoethanol, and 100-μg/mL kanamycin, was used throughout. MEM (Sigma) with or without FBS was used in some procedures.

Reagents

Stock solutions of cerivastatin (Bayer) and pravastatin (Wako Pure Chemical Industries, Ltd) were prepared in distilled water. Stock solutions of atorvastatin (Pfizer), simvastatin (Wako Pure Chemical Industries, Ltd), and lovastatin (Wako Pure Chemical Industries, Ltd) were made in dimethyl sulfoxide. The stocks were diluted to working solutions in culture medium for in vitro experiments or in saline for in vivo experiments. The nominal concentrations of dimethyl sulfoxide in the working solutions used in the in vitro experiments were 0.005% for atorvastatin and simvastatin and 0.01% for lovastatin. Mevalonate was purchased from Sigma.

Cell Preparations

$CD4^+$ T cells were prepared from the spleens of C57BL/6 or BALB/c mice as described previosuly.[13] Briefly, spleen cells depleted of red blood cells by treatment with Tris-buffered NH_4Cl (pH 7.4) were passed through a nylon wool column, followed by depletion of $CD8^+$, $I\text{-}E^+$, $Fc\gamma RII/III^+$, or $CD24^+$ cells on a MACS column (Miltenyi Biotech). The recovered cells were confirmed to be >95% $CD4^+$ and were used as naive $CD4^+$ T cells. T cell–depleted spleen cells were prepared from the spleen as described[13] and used as APC after 35-Gy irradiation.

In Vitro Priming of Naive $CD4^+$ T Cells

Priming of naive $CD4^+$ T cells (2×10^5 cells/2 mL per culture) was carried out using 1 μg/mL anti-CD3 monoclonal antibody (mAb) (145-2C11) with irradiated T cell–depleted spleen cells (3×10^6 cells/2 mL per culture) in wells of a 24-well plate (Iwaki Glass Co). In some experiments, naive $CD4^+$ T cells were primed with plate-coated anti-CD3 mAb (2 μg/mL, 145-2C11) and anti-CD28 mAb (2 μg/mL, 37.51). Cultures received only medium or 0.01 to 30 μmol/L statins. In addition, some cultures were supplemented with 5 μg/mL anti–IL-4 mAb (11B11) and 1000 U/mL IL-12 (rmIL-12, Genetic Institute) (Th1 polarizing condition). On day 4, $CD4^+$ T cells primed as described above were distributed into four wells in fresh medium containing 2.5 ng/mL IL-2 (rhIL-2, Ajinomoto Co). On day 6, $CD4^+$ T cells were recovered by a centrifugation over Ficoll and restimulated at 1×10^6 cells/mL with 50 ng/mL phorbol 12-myristate 13-acetate (PMA) and 1 μmol/L ionomycin for 5 hours in the presence of 5 μg/mL brefeldin A for the last 3 hours of culture.

Intracellular Cytokine Staining

The T cells, restimulated as described above, were stained with biotin–anti-CD4 mAb in the presence of anti-FcR mAb (2.4G2) followed by incubation with streptavidin-Cychrome. They were then fixed with 4% paraformaldehyde in PBS and permeabilized with 0.1% saponin. Subsequently, they were incubated with FITC–anti-IFN-γ mAb (PharMingen) and PE–anti-IL-4 mAb (PharMingen) in the presence of 0.1% saponin for 1 hour at 4°C. The cells were gated on $CD4^+$ cells to exclude any residual APC and subjected to two-color analysis on a FACScan (Becton Dickinson). FITC- or PE-conjugated isotype-matched control mAbs were used as negative controls to set quadrant markers.

In Vivo Priming of T Cells

C57BL/6 or BALB/c mice were immunized subcutaneously with 100 μg ovalbumin (OVA) (Sigma) emulsified in CFA (Difco Laboratories). They were also injected intraperitoneally with either saline or 2 to 10 mg/kg cerivastatin in a volume of 100 μL per mouse on days −1, 0, 1, 2, 3, and 4. On day 9, single-cell suspension of subinguinal lymph node cells (LNCs) was cultured at 2×10^6 cells/1 mL per culture in 24-well plates or at 1×10^6 cells/250 μL per culture in 48-well plates in the presence of 500 μg/mL OVA. Culture supernatants were harvested after 72 hours and stored at −30°C until assayed for cytokines by ELISA.

Cytokine ELISA

IL-4 and IFN-γ in culture supernatants were assayed by ELISA, as described previously,[14] using paired mAbs specific for the corresponding cytokine. The lower detection limits of these assays were as follows: IL-4, 6 pg/mL; IFN-γ, 100 pg/mL.

Functional and Morphological Analyses of the Kidney of C57BL/6 Mice

On the last 2 days of the study of in vivo priming of T cells, a 24-hour urine specimen was collected, and the urine collected on the last day was used for determination of urinary excretions of protein. The concentration of protein in urine was determined using protein assay (BioRad).[15] At the time the mice were killed, the right kidney was obtained for morphological evaluation.

To assess the extent of injured glomerular capillaries, we semiquantitatively determined the area of the glomerulus having capillary damage. The severity of these lesions was graded according to the percentage of the glomeruli involved, as follows: 0, no lesions; 1+, 1% to 25%; 2+, 26% to 50%; 3+, 51% to 75%; and 4+, 76% to 100%. An overall glomerulosclerosis index was calculated by multiplying the severity score (0 to 4+) by the percentage of glomeruli affected and totaling the five values.

To assess the accumulation of mesangial matrix in the glomerulus, we used RGB color analysis of glomerular mesangium stained by periodic acid Schiff reagent and determined the areas showing the same pattern of RGB wavelength as the mesangium using an Olympus microscope and WinRoof color analyzing software (Mitani Corp) according to the previous method.[16] The measurement was expressed as the percentage of mesangial matrix to the whole area of a glomerulus tested. We scanned 100 glomeruli per each mouse.

Statistical Analysis

Results are expressed as mean±SEM. Student's t tests and one-way ANOVA were performed with STATISTICA software (StatSoft) and a Windows 98 computer system. Differences between groups were considered significant at $P<0.05$.

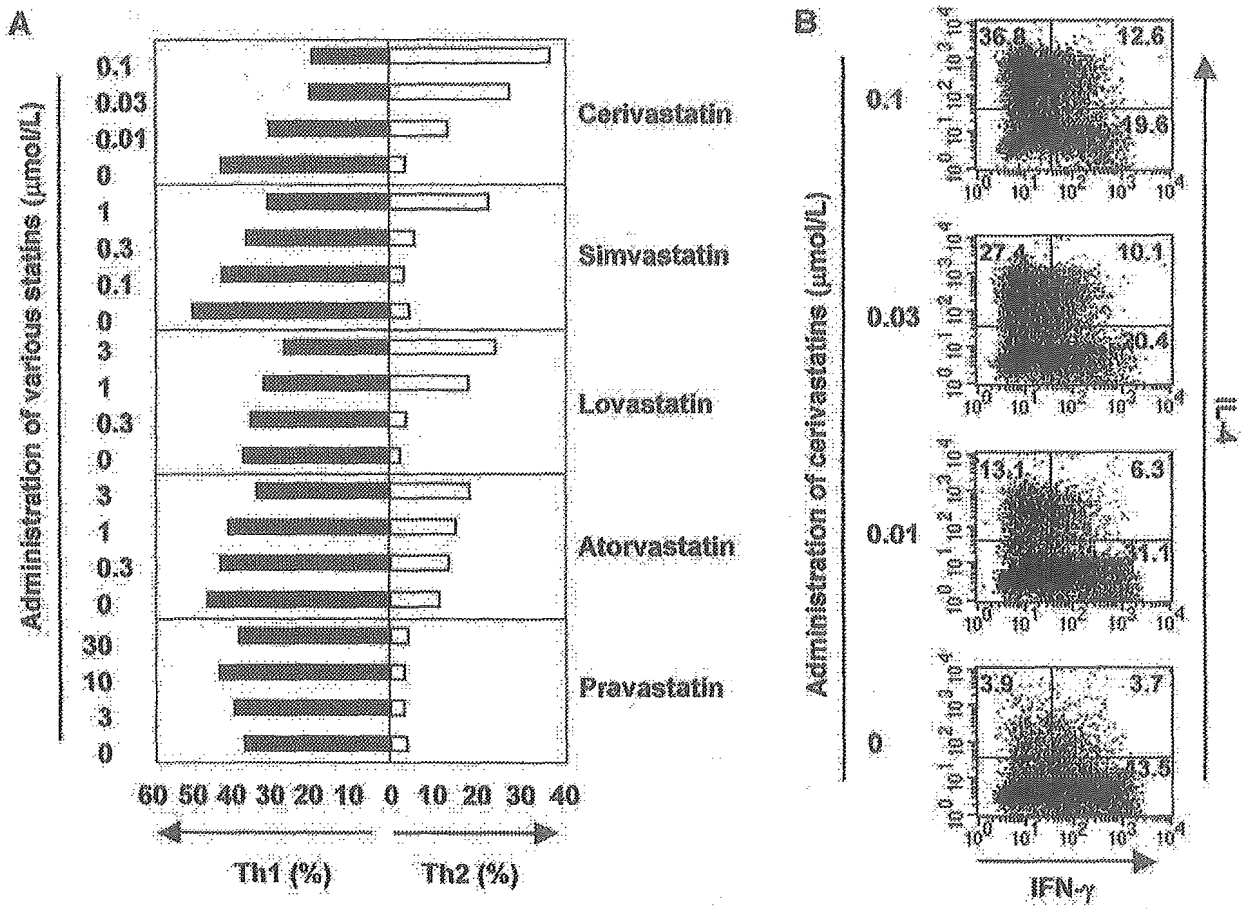

Figure 1. Cytokine production profiles of CD4+ T cells primed in vitro in the presence of various statins. Flow cytometric analysis of intracellular IL-4 and INF-γ staining of CD4+ T cells from C57BL/6 mice primed with anti-CD3 mAb and T cell–depleted spleen cells in the absence or presence of various statins, as indicated. A, Proportions of Th1 (filled bars) and Th2 cells (open bars) obtained from flow diagrams of experiments using cerivastatin, simvastatin, lovastatin, atorvastatin, or pravastatin. B, Representative flow diagrams of experiments using cerivastatin. The annotated numbers indicate the percentages of cells in each quadrant. Each experiment was performed 3 times, and representative data are shown.

Results

Statins Inhibit Th1 Development and Promote Th2 Development In Vitro

To study the effect of statins on Th polarization, naive CD4+ T cells from C57BL/6 mice were primed with anti-CD3 mAb together with irradiated T cell–depleted spleen cells as APCs in the absence or presence of various concentrations of statins, ie, cerivastatin, simvastatin, lovastatin, atorvastatin, and pravastatin. Six days later, the phenotypes of Th cells generated were assayed by intracellular staining of IFN-γ and IL-4 on restimulation with PMA and ionomycin. As shown in Figure 1A, any of the statins except pravastatin dose-dependently inhibited Th1 development and promoted Th2 development, resulting in the promotion of Th2 polarization. Cerivastatin exhibited the most remarkable Th2 polarization effect considering the dose-response relationship.

To determine whether the enhancement of Th2 polarization by statins is limited to Th1-prone C57BL/6 mice (Figure 1B) or could be reproduced in Th2-prone BALB/c mice,[17] naive CD4+ T cells from BALB/c mice were primed in the absence or presence of 0.01 to 0.1 μmol/L cerivastatin. Naive CD4+ T cells from BALB/c mice developed predominantly Th2 cells, and the Th2 development was additionally enhanced by 0.01 μmol/L or more of cerivastatin (Figure 2). On the other hand, because Th1 cells were scarcely detected even in the absence of cerivastatin, we could not detect significant suppression of Th1 development by cerivastatin.

In addition, as shown in Figure 3, the enhanced Th2 polarization by cerivastatin was reversed by the addition of mevalonate, the immediate downstream metabolite of HMG-CoA. The addition of increasing doses of mevalonate evidently attenuated both the inhibition of Th1 and augmentation of Th2 development by cerivastatin, and 0.3 mmol/L or more of mevalonate completely reversed the effects of cerivastatin. Taken together, these results indicate that statins promote Th2 polarization irrespective of genetic background of mice strain and the effect is related to their class effects of inhibitors of HMG-CoA reductase.

Cerivastatin Has Direct Effects on Naive CD4+ T Cells, Resulting in Suppression of Th1 Development

To determine whether statins directly affect Th development independently of APC, naive CD4+ T cells were primed with plate-bound anti-CD3 mAb plus anti-CD28 mAb in the absence of APC together with or without 0.1 μmol/L ceriv-

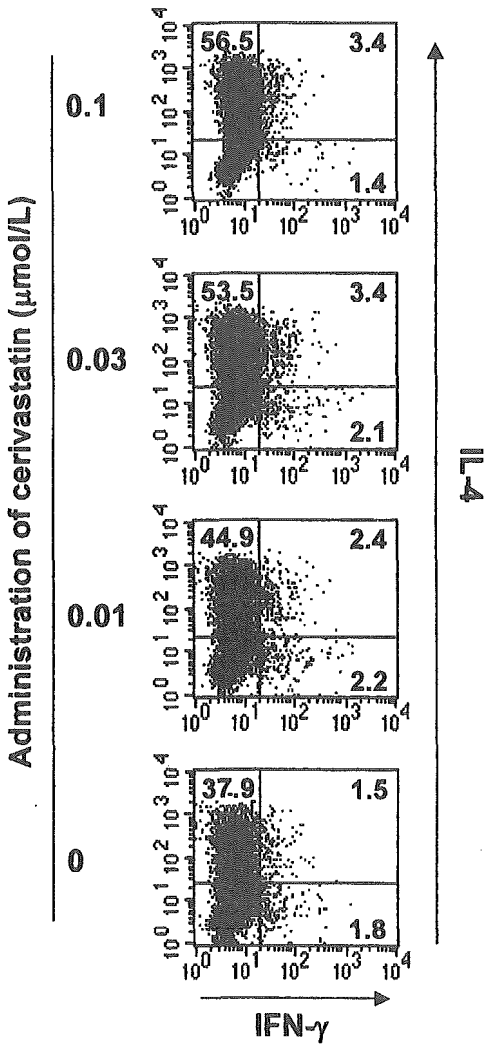

Figure 2. Cytokine production profiles of CD4+ T cells from BALB/c mice primed in vitro in the presence of cerivastatin. Flow cytometric analysis of intracellular IL-4 and IFN-γ staining of CD4+ T cells from BALB/c mice primed with anti-CD3 mAb and T cell–depleted spleen cells in the absence or presence of 0.01 to 0.1 μmol/L cerivastatin. The annotated numbers indicate the percentages of cells in each quadrant. The data shown are representative of 3 experiments with similar results.

astatin. Although the proportion of Th1 cells developed in culture driven by plate-bound anti-CD3 mAb plus anti-CD28 mAb was significantly higher than that developed in culture with anti-CD3 mAb and APC (72.9% versus 38.8%), cerivastatin significantly suppressed Th1 development by 45% (72.9% and 40.0%) (Figures 4A and 4B). These results suggest that naive CD4+ T cells can be direct targets for the effect of statins on Th1 development.

On the other hand, Th2 cells were scarcely generated in the absence of APC, and cerivastatin did not augment Th2 development (Figure 4B). Therefore, the effect of cerivastatin on the enhancement of Th2 development seems to be mediated by modulation of APC functions. It has been reported that statins downregulate MHC class II, CD80, CD86, and CD40 expression on APC,[8,10] all of which promote Th2 development.[1,2,18,19] However, the expression of these molecules on APC in the presence of cerivastatin remained unchanged (Figure 5).

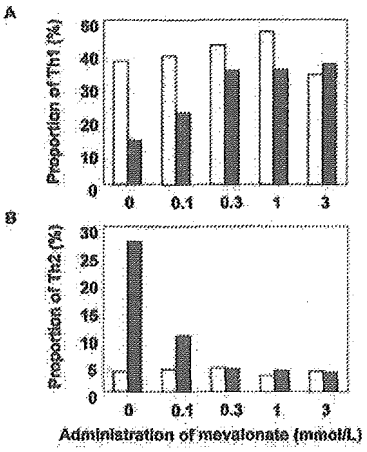

Figure 3. Effect of mevalonate on cerivastatin-induced Th2 polarization. Flow cytometric analysis of intracellular IL-4 and IFN-γ staining of CD4+ T cells from C57BL/6 mice primed with anti-CD3 mAb and T cell–depleted spleen cells in the absence (open bars) or presence (filled bars) of 0.03 μmol/L cerivastatin together with increasing concentrations of mevalonate. Results are expressed as percentages of Th1 (A) and Th2 cells (B). Data shown are representative of 3 experiments with similar results.

Cerivastatin Does Not Induce Apoptosis in Th1

As for the mechanism of the Th2 polarization induced by statins, we were unable to neglect the contribution of selective apoptosis in Th1 cells. To examine this possibility, the proportion of apoptotic cells within CD4+ T cells cultured for 4 days with anti-CD3 mAb and APC in the absence or presence of 0.1 μmol/L cerivastatin was assessed by Annexin V staining. The percentage of Annexin V+ cells in the CD4+ T cell population remained unchanged by the addition of cerivastatin (9.7±0.5% and 9.9±1.1% in the presence and absence of cerivastatin, respectively). Furthermore, when naive CD4+ T cells were primed under the condition where Th1 polarization was promoted (anti–IL-4 mAb plus IL-12), Th1 development was not suppressed by cerivastatin (Figure 4C). Taken together, these results indicate that the suppression of Th1 development by cerivastatin is not attributable to a selective induction of apoptosis in Th1.

Cerivastatin Suppresses Th1 Development In Vivo

To test whether cerivastatin has similar effects in vivo, cytokine production profiles of draining LNCs from mice immunized with OVA and treated with cerivastatin were assessed. As shown in Figure 6, cerivastatin treatment suppressed IFN-γ production of LNCs from both C57BL/6 and BALB/c mice after restimulation with OVA ex vivo. LNCs from C57BL/6 mice immunized with OVA did not produce detectable IL-4, which is consistent with results reported,[20] and cerivastatin treatment did not augment IL-4 production (data not shown). On the other hand, LNCs from BALB/c mice immunized with OVA and restimulated with OVA ex vivo produced detectable IL-4. However, the IL-4 production of LNCs was not augmented by cerivastatin treatment (data not shown). The suppression of IFN-γ production by the

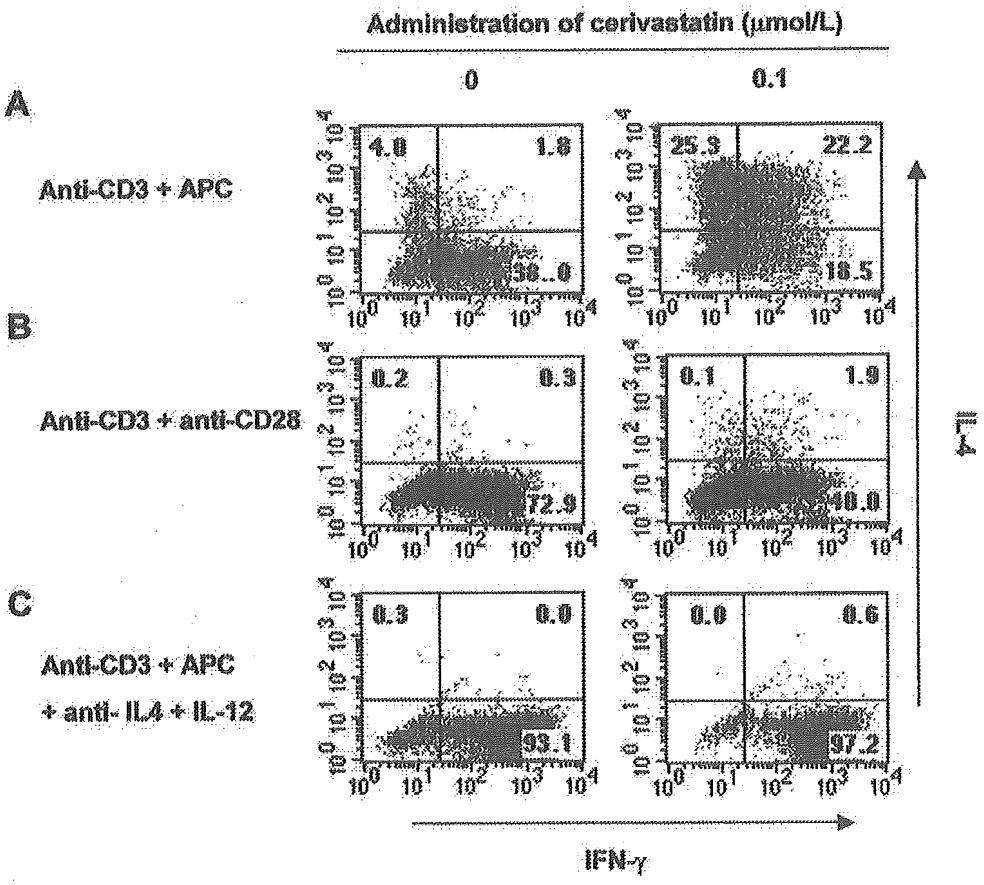

Figure 4. No requirement of APC for the suppression of Th1 development by cerivastatin. Flow cytometric analysis of intracellular IL-4 and IFN-γ staining of $CD4^+$ T cells from C57BL/6 mice primed in the presence or absence of APC. $CD4^+$ T cells were primed with anti-CD3 mAb and T cell–depleted spleen cells in the absence (A) or presence of anti–IL-4 mAb and IL-12 (C). $CD4^+$ T cells were also primed with plate-coated anti-CD3 mAb and anti-CD28 mAb (B). Cultures received medium alone or 0.1 μmol/L cerivastatin. Data shown are representative of 3 experiments with similar results.

treatment with cerivastatin was not attributable to the alteration of cell composition within LNCs, because the numbers of total LNCs and the proportion of $CD4^+$, Mac-1^+, or $B220^+$ cells in cerivastatin-treated mice were essentially equal to those in untreated mice (data not shown).

Cerivastatin Ameliorates Functional and Morphological Alterations in the Kidney

To assess pathophysiological role of the alterations of Th polarization induced by statins for organ injury in immune-related diseases, we investigated the effects of cerivastatin on functional and morphological alterations in the kidney of C57BL/6 mice immunized with OVA emulsified with CFA. In this model, urinary excretion of protein was significantly higher in C57BL/6 mice immunized with OVA/CFA (control) group than the untreated mice without immunization (0.72 ± 0.17 versus 0.35 ± 0.11 mg/dL, $P<0.001$). This increase was significantly decreased by 20% in mice treated with 10 mg/kg cerivastatin (0.59 ± 0.16 mg/dL, $P<0.05$) (Figure 7).

In untreated mice, the glomeruli of the kidney exhibited an apparently normal appearance (Figure 8A). The interstitium was not expanded. In contrast, in untreated, immunized mice, the glomerulus exhibited a significant expansion of mesangial matrix with an increase in number of mesangial cells (areas indicated by arrows) (Figure 8B) along with normal tubules (Figure 8C). In the immunized mice treated with cerivastatin, proliferation of mesangial cells decreased and the areas of mesangium became small (Figure 8D).

The improvement of glomerular injury was assessed using two different methods. As shown in Figure 8E, overall glomerulosclerosis index significantly decreased in cerivastatin-treated mice compared with the untreated, immunized group. Moreover, the mesangial area determined by RGB wavelength analyses was significantly lower in the cerivastatin-treated group than the immunized mice without treatment (Figure 8F).

In this model, plasma total cholesterol levels of mice treated with 10 mg/kg cerivastatin (89.4 ± 5.0 mg/dL) were never different from those of the control group (86.7 ± 4.9 mg/dL, $P=0.23$).

Discussion

In the present study, we demonstrate that four statins, cerivastatin, simvastatin, lovastatin, and atorvastatin, promote Th2 polarization via suppression of Th1 development and augmentation of Th2 development from naive $CD4^+$ T cells primed with anti-CD3 mAb and splenic APC in vitro. Considering the dose-response relationship, cerivastatin exhibited the most potent effect on Th2 polarization. This effect

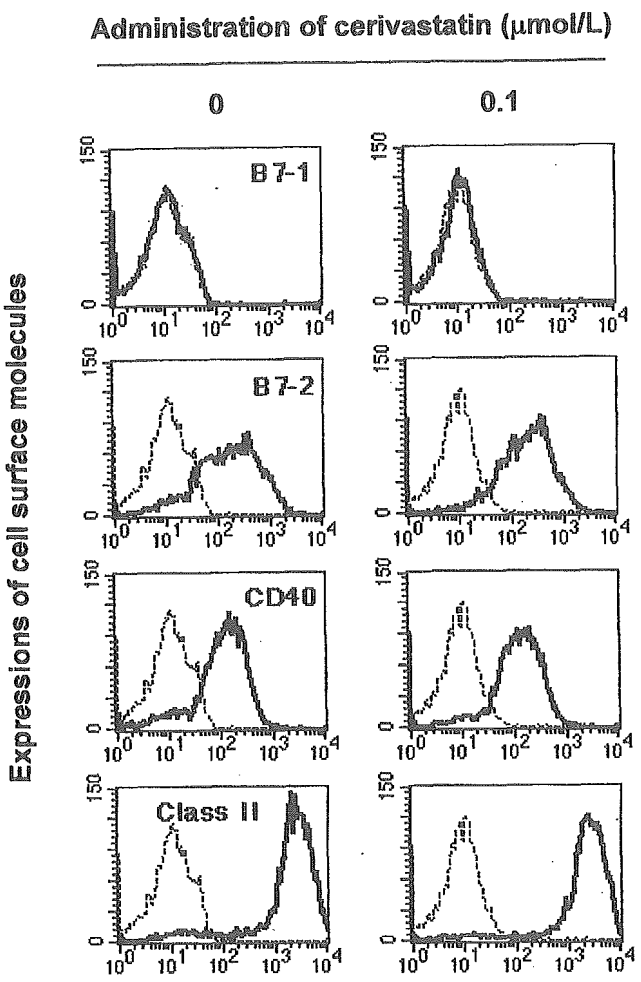

Figure 5. Expression of MHC class II and costimulatory molecules on APCs. C57BL/6 mice spleen cells depleted of T cells (3×10^6 cells/2 mL per culture) were cultured with syngenic $CD4^+$ T cells (2×10^5 cells/2 mL per culture) in the presence of 1 μg/mL anti-CD3 mAb for 4 days. The expressions of B7-1, B7-2, CD40, and MHC class II molecules on $Fc\gamma R^+$ cells were analyzed by two-color flow cytometry.

was seen in two genetic backgrounds, C57BL/6 and BALB/c mice that are prone to develop Th1 and Th2, respectively,[17] and was completely abrogated by the addition of mevalonate, the immediate downstream metabolite of HMG-CoA. These findings indicate that the effects of these statins are attributable to a class-effect of inhibitors of HMG-CoA reductase and indebted to mevalonate depletion.

Statins have been shown to suppress production of IL-12[10,11] that plays a pivotal role in Th1 development.[2] Therefore, APC can be the target for the immunomodulatory activities of statins. However, our analysis in this study revealed that statins also had a direct effect on naive $CD4^+$ T cells on TCR stimulation, thereby resulting in an inhibition of Th1 development. Inhibition of Th1 development was also seen even when naive $CD4^+$ T cells were primed with plate-coated anti-CD3 and anti-CD28 mAbs in the absence of APC. This inhibition of Th1 development was not attributable to the selective induction of apoptosis in Th1 cells, which is in accord with previous studies.[10–12] Recently, it has been shown that STAT4 phosphorylation in T cells from experimental autoimmune encephalomyelitis mice was reduced by atorvastatin.[10] Therefore, it is possible that statins directly affect STAT4 signaling pathway, resulting in the inhibition of Th1 development.[21] It also has been shown that atorvastatin inhibits activation of nuclear factor-κB,[22] which preferentially promotes Th1 development.[23] Therefore, it is possible that statins inhibit Th1 development via attenuation of nuclear factor-κB signaling in naive $CD4^+$ T cells. Alternatively, statins might weaken the strength of signals delivered by TCR via modulation of cholesterol microdomains, which has been shown to suppress Th1 development.[2,24,25]

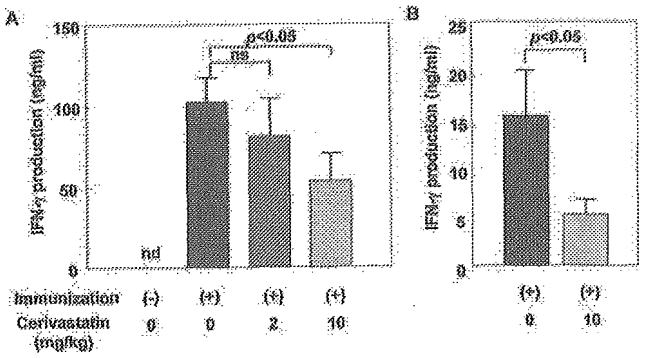

Figure 6. Suppression of IFN-γ production by lymph node T cells in cerivastatin-treated mice. C57BL/6 (A) or BALB/c (B) mice immunized with 100 μg OVA in CFA were injected intraperitoneally with saline or cerivastatin at concentrations of 2 or 10 mg/kg on days −1, 0, 1, 2, 3, and 4. Nine days after immunization, draining lymph node cells (2×10^6 cells/1 mL per culture) were cultured in the presence of 500 μg/mL OVA for 72 hours. IFN-γ in the culture supernatants was assessed by ELISA. Values were expressed as mean±SEM of 8 to 12 mice. *P* values between control and 10 mg/kg cerivastatin groups were assessed using Student's *t* test. ND indicates not detectable; NS, not significant.

On the other hand, the enhancement of Th2 development by statins was indicated to be mediated by modulation of APC functions. Augmentation of Th2 development was seen only when naive $CD4^+$ T cells were primed in the presence of APC. Statins have been demonstrated to bind to the LFA-1 L-site that is critical to intercellular adhesion molecule-1 binding,[9] and blocking of LFA-1/intercellular adhesion

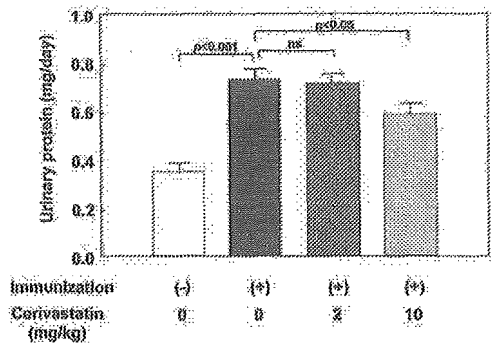

Figure 7. Effect of cerivastatin on the kidney function. C57BL/6 mice were immunized as described in the text. Twenty-four-hour collected urine on day 9 was used for determination of urinary protein excretions. The *P* value between control and 10 mg/kg cerivastatin groups was assessed using Student's *t* test. NS indicates not significant.

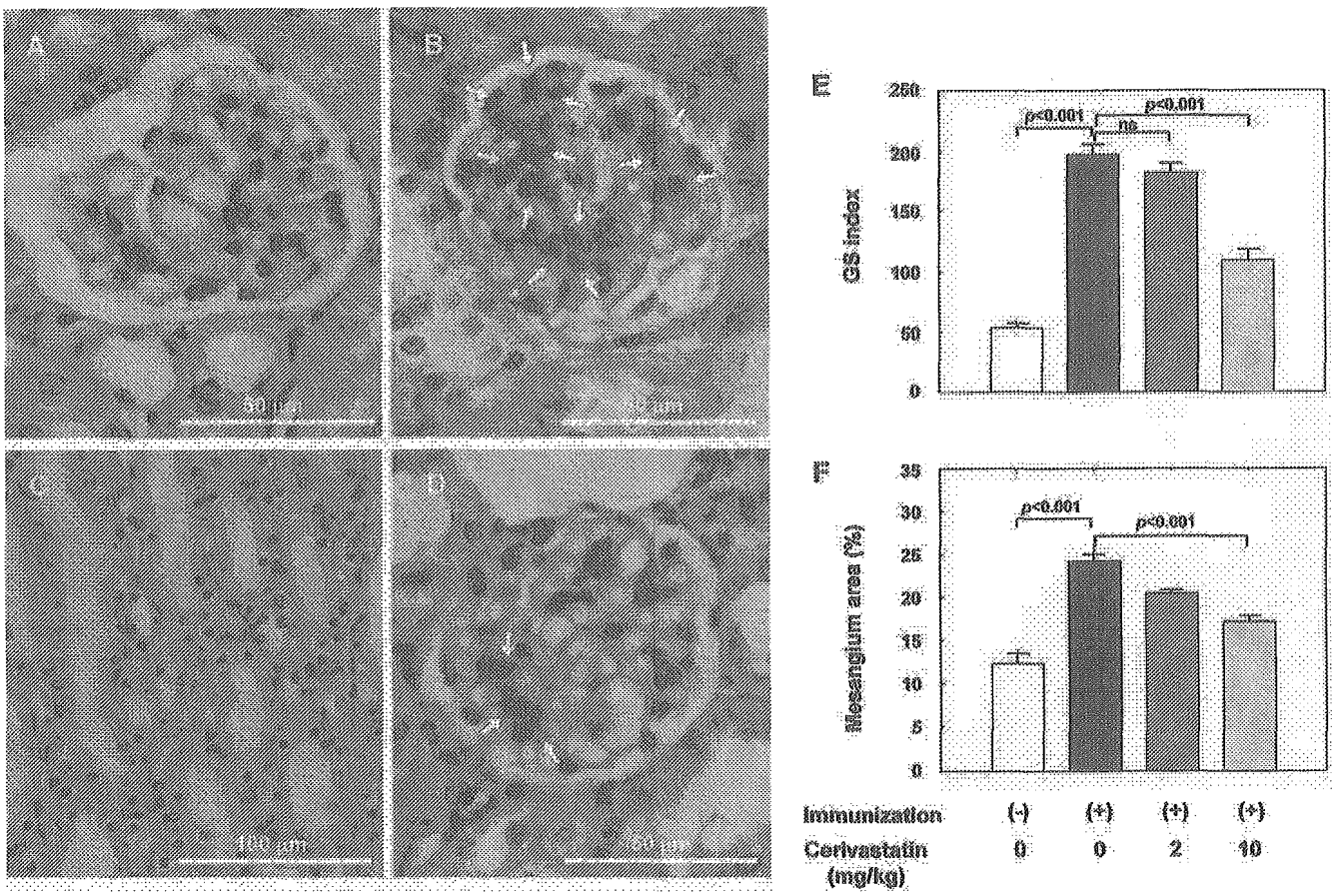

Figure 8. Effect of cerivastatin on the morphological alterations in the kidney. C57BL/6 mice were immunized as described in the text. Kidneys were obtained on day 9 after immunization. Half of the kidney was immediately fixed in 3.5% formalin, and sagittal slices were cut and embedded in paraffin. Sections 2 μm in thickness were cut and stained with periodic acid Schiff stains. Glomerulus from an untreated and unimmunized mouse (A) and a glomerulus from an immunized mouse without cerivastatin treatment (control) (B). Arrows indicate area of mesangial expansion. C, Renal tubules of the same kidney shown in B. D, Glomerulus from immunized mice with 10 mg/kg cerivastatin treatment. E, Glomerulosclerosis (GS) index. Data are expressed as mean±SEM. The *P* value between control and 10 mg/kg cerivastatin groups was assessed using Student's *t* test. F, Mesangial expansion in glomerulus was assessed by RGB color analysis. Data are expressed as mean±SEM. The *P* value among control and 2 and 10 mg/kg cerivastatin groups was assessed using one-way ANOVA. NS indicates not significant.

molecule-1 interaction has been shown to promote Th2 development.[26] Therefore, it is also possible that blocking of LFA-1–mediated T cell costimulation by statins might promote Th2 development. On the other hand, statins have been reported to downregulate the expressions of MHC class II, CD40, CD80, and CD86 on APC induced by IFN-γ.[8,10] In this study, however, the expressions of these molecules on APCs interacting with naive $CD4^+$ T cells in the presence of anti-CD3 mAb were not suppressed by statins (Figure 5). Similarly, Leung et al[12] have also demonstrated that simvastatin treatment did not affect MHC class II expression. Accordingly, the expressions of these molecules seemed not to play an important part in the enhanced Th2 development by statins. Modulation of cytokine production by APC could be another candidate of the mechanism for inducing Th2 development. Additional research will be required to elucidate the mechanisms involved in the effects of statins on Th1/Th2 development.

Among the statins tested, only pravastatin did not behave as a modulator of Th1/Th2 balance. The reason for the negative findings of pravastatin is not clear; however, it may be attributable to its lipophobic properties that hinder the translocation of pravastatin across the cell membranes.

In accordance with results obtained in in vitro experiments, OVA-specific IFN-γ production of draining LNCs from C57BL/6 and BALB/c mice immunized with OVA was suppressed by cerivastatin treatment. The mice were inoculated with CFA, an oil that contains inactivated mycobacteria, and this was a standard procedure for inducing antigen-specific Th1 development.[27] Thus, cerivastatin alters Th1/Th2 balance mainly through inhibition of Th1 response, even in potent Th1-provoking circumstances. These results accord with recent studies showing that atorvastatin[10,11] or simvastatin[12] is capable of inhibiting Th1 responses in murine autoimmune models. In the present study, in vitro Th2 development was clearly enhanced by cerivastatin; however, Th2 development was not significantly altered in ex vivo study. This failure to promote Th2 development is consistent with previous data on simvastatin.[12] Considering these data, statins conceivably inhibit Th1 development without enhancing compensatory Th2 development in vivo.

More interestingly, we clearly demonstrated that the treatment with cerivastatin was associated with a significant improvement of morphological injury in glomeruli and a decrease in proteinuria in OVA-immunized mice. These effects were not associated with cholesterol reduction. The decrease of glomerular sclerosis by cerivastatin treatment was positively related to the suppression of IFN-γ–producing Th1 response in draining LNCs (r=0.54, P<0.05). These results strongly suggest that the Th1/Th2 alterations and the following changes of cytokines expression might be responsible for the attenuation of inflammatory lesions in the glomeruli. In fact, recent studies have found that Th1 cells may be more important in mediating glomerular sclerosis than humoral factors related to immune mechanism.[28–30] Furthermore, Radeke et al[28] have shown that OVA-specific Th1 cells alone are sufficient to induce glomerulonephritis together with antigen by using SCID mice lacking humoral immunity. Taken together, it seems highly possible that cerivastatin treatment protects renal glomeruli against inflammatory process, probably through inhibition of Th1 response. In fact, it is well-known that statins have demonstrated beneficial effects in different models of progressive renal dysfunction, and part of the benefit is actually independent of the lipid-lowering effect.[31] The non–lipid-mediated mechanisms consist of inhibition of chemokines, such as monocyte chemoattractant protein-1,[32] and reduction of proliferation of mesangial cells,[33,34] renal epithelial tubular cells,[35] and vascular smooth muscle cells.[36,37]

Finally, our present results, if combined with data reported by other investigators,[10–12] provide evidence that the beneficial effects of statins on the inflammatory diseases are mediated, at least in part, by the inhibition of Th1 development. The suppression of IFN-γ production of LNCs by cerivastatin treatment was associated with reduced mesangial matrix expansion of glomeruli of the kidney and attenuation of proteinuria, suggesting that HMG-CoA reductase inhibitors regulate in vivo the Th1/Th2 polarization and that such an immune-related mechanism possibly plays a role in improvement of the immune-induced glomerular injury with treatment of statins.

Acknowledgments

The study was supported in part by a Grant-in-Aid for Encouragement of Young Scientist from the Ministry of Education, Culture, Sports, Science, and Technology, Japan (13770185). The authors express great thanks to Bayer, Wuppertal, Germany, and Pfizer, Sandwich, UK, for their kind gifts of cerivastatin and atorvastatin, respectively.

References

1. Abbas AK, Murphy KM, Sher A. Functional diversity of helper T lymphocytes. *Nature.* 1996;383:787–793.
2. Constant SL, Bottomly K. Induction of Th1 and Th2 CD4+ T cell responses: the alternative approaches. *Annu Rev Immunol.* 1997;15:297–322.
3. Romagnani S. Th1 and Th2 in human diseases. *Clin Immunol Immunopathol.* 1996;80:225–235.
4. Randomised trial of cholesterol lowering in 4444 patients with coronary heart disease: the Scandinavian Simvastatin Survival Study (4S). *Lancet.* 1994;19;344:1383–1389.
5. Takemoto M, Liao JK. Pleiotropic effects of 3-hydroxy-3-methylglutaryl coenzyme A reductase inhibitors. *Arterioscler Thromb Vasc Biol.* 2001;21:1712–1719.
6. Koh KK. Effects of statins on vascular wall: vasomotor function, inflammation, and plaque stability. *Cardiovasc Res.* 2000;47:648–657.
7. Ridker PM, Rifai N, Clearfield M, Downs JR, Weis SE, Miles JS, Gotto AM Jr, for the Air Force/Texas Coronary Atherosclerosis Prevention Study Investigators. Measurement of C-reactive protein for the targeting of statin therapy in the primary prevention of acute coronary events. *N Engl J Med.* 2001;28;344:1959–1965.
8. Kwak B, Mulhaupt F, Myit S, Mach F. Statins as a newly recognized type of immunomodulator. *Nat Med.* 2000;6:1399–1402.
9. Weitz-Schmidt G, Welzenbach K, Brinkmann V, Kamata T, Kallen J, Bruns C, Cottens S, Takada Y, Hommel U. Statins selectively inhibit leukocyte function antigen-1 by binding to a novel regulatory integrin site. *Nat Med.* 2001;7:687–692.
10. Youssel S, Stuve O, Patarroyo JC, Rulz PJ, Radosevich JL, Hur EM, Bravo M, Mitchell DJ, Sobel RA, Steinman L, Zamvil SS. The HMG-CoA reductase inhibitor, atorvastatin, promotes a Th2 bias and reverses paralysis in central nervous system autoimmune disease. *Nature.* 2002;420:78–84.
11. Aktas O, Waiczies S, Smorodchenko A, Dorr J, Seeger B, Prozorvski T, Sallach S, Endres M, Brocke S, Nitsch R, Zipp F. Treatment of relapsing paralysis in experimental encephalomyelitis by targeting Th1 cells through atorvastatin. *J Exp Med.* 2003;197:725–733.
12. Leung BP, Sattar N, Crilly A, Prach M, McCarey DW, Payne H, Madhok R, Campbell C, Gracie JA, Liew FY, McInnes IB. A novel anti-inflammatory role for simvastatin in inflammatory arthritis. *J Immunol.* 2003;170:1524–1530.
13. Hakamada-Taguchi R, Kato T, Ushijima H, Murakami M, Uede T, Nariuchi H. Expression and co-stimulatory function of B7-2 on murine CD4+ T cells. *Eur J Immunol.* 1998;28:865–873.
14. Kato T, Nariuchi H. Polarization of naive CD4+ T cells toward the Th1 subset by CTLA-4 costimulation. *J Immunol.* 2000;164:3554–3562.
15. Uehara Y, Kawabata Y, Hirawa N, Takada S, Nagata T, Numabe A, Iwai J, Sugimoto T. Possible radical scavenging properties of cicletanine and renal protection in Dahl salt sensitive rats. *Am J Hypertens.* 1993;6:463–472.
16. Numabe A, Ara N, Hakamada-Taguchi R, Suzuki N, Hirawa N, Kawabata Y, Negoro T, Nagata T, Goto A, Toyo-oka T, Fujita T, Uehara Y. Effects of anti-platelet aggregation drug dilazep on cognitive function in Dahl salt sensitive rats. *Hypertens Res.* 2003;26:185–191.
17. Bix M, Wang ZE, Thiel B, Schork NJ, Locksley RM. Genetic regulation of commitment to interleukin 4 production by a CD4+ T cell-intrinsic mechanism. *J Exp Med.* 1998;188:2289–2299.
18. Sayegh MH, Akalin E, Hancock WW, Russell ME, Carpenter CB, Linsley PS, Turka LA. CD28-B7 blockade after alloantigenic challenge in vivo inhibits Th1 cytokines but spares Th2. *J Exp Med.* 1995;181:1869–1874.
19. Stuber E, Strober W, Neurath M. Blocking the CD40L-CD40 interaction in vivo specifically prevents the priming of T helper 1 cells through the inhibition of interleukin 12 secretion. *J Immunol.* 1996;183:693–698.
20. Karulin AY, Hesse MD, Yip HC, Lehmann PV. Indirect IL-4 pathway in type 1 immunity. *J Immunol.* 2002;168:545–553.
21. Farrar JD, Asnagli H, Murphy KM. T helper subset development: roles of instruction, selection, and transcription. *J Clin Invest.* 2002;109:431–435.
22. Ortego M, Bustos C, Hernandez-Presa MA, Tunon J, Diaz C, Hernandez G, Egido J. Atorvastatin reduces NF-κB activation and chemokine expression in vascular smooth muscle cells and mononuclear cells. *Atherosclerosis.* 1999;147:253–261.
23. Aronica MA, Mora AL, Mitchell DB, Finn PW, Johnson JE, Sheller JR, Boothby MR. Preferential role for NF-κB/Rel signaling in the type 1 but not type 2 T cell-dependent immune response in vivo. *J Immunol.* 1999;163:5116–5124.
24. Balamuth F, Leitenberg D, Unternaehrer J, Mellman I, Bottomly K. Distinct patterns of membrane microdomain partitioning in Th1 and Th2 cells. *Immunity.* 2001;15:729–738.
25. Gubina E, Chen T, Zhang L, Lizzio EF, Kozlowski S. CD43 polarization in unprimed T cells can be dissociated from raft coalescence by inhibition of HMG CoA reductase. *Blood.* 2002;99:2518–2525.
26. Salomon B, Bluestone JA. LFA-1 interaction with ICAM-1 and ICAM-2 regulates Th2 cytokine production. *J Immunol.* 1998;161:5138–5142.
27. Yip HC, Karulin AY, Tary-Lehmann M, Hesse MD, Radeke H, Heeger PS, Trezza RP, Heinzel FP, Forsthuber T, Lehmann PV. Adjuvant-guided type-1 and type-2 immunity: infectious/noninfectious dichotomy defines the class of response. *J Immunol.* 1999;162:3942–3949.
28. Radeke HH, Tschering T, Karulin A, Schumm G, Emancipator SN, Resch K, Tary-Lehmann M. CD4+ T cells recognizing specific antigen

deposited in glomeruli cause glomerulonephritis-like kidney injury. *Clin Immunol.* 2002;104:161–173.
29. Wu J, Hicks J, Borillo J, Glass WF II, Lou Y-H. $CD4^+$ T cells specific to a glomerular basement membrane antigen mediate glomerulonephritis. *J Clin Invest.* 2002;109:517–524.
30. Huang XR, Tipping PG, Shuo L, Holdsworth SR. Th1 responsiveness to nephritogenic Ags determines susceptibility to crescentic glomerulonephritis in mice. *Kidney Int.* 1997;51:94–103.
31. Oda H, Keane WF. Recent advances in statins and the kidney. *Kidney Int.* 1999;56:S2–S5.
32. Kim SY, Guijarro C, O'Donnell MP, Kasiske BL, Kim Y, Keane WF. Human mesangial cell production of monocyte chemoattractant protein-1: modulation by lovastatin. *Kidney Int.* 1995;48:363–371.
33. O'Donnnell MP, Kasiske BL, Kim Y, Atluru D, Keane WF. Lovastatin inhibits proliferation of rat mesangial cells. *J Clin Invest.* 1993;91:83–87.
34. Grandaliano G, Biswas P, Choudhury GG, Abboud HE. Simvastatin inhibits PDGF-induced DNA synthesis in human glomerular mesangial cells. *Kidney Int.* 1993;44:503–508.
35. Vrtovsnik F, Couette S, Prie D, Lallemand D, Friedlander G. Lovastatin-induced inhibition of renal epithelial tubular cell proliferation involves a p21ras activated, AP-1-dependent pathway. *Kidney Int.* 1993;44:503–508.
36. Rogler G, Lackner KJ, Schmitz G. Effects of fluvastatin on growth of porcine and human vascular smooth muscle cells in vitro. *Am J Cardiol.* 1995;76:114A–116A.
37. Munro E, Patel M, Cha P, Betteridge L, Clunn G, Gallagher K, Hughes A, Schachter M, Wolfe J, Sever P. Inhibition of human vascular smooth muscle cell proliferation by lovastatin: the role of isoprenoid intermediates of cholesterol synthesis. *Eur J Clin Invest.* 1994;24:766–772.

Am J Physiol Endocrinol Metab 285: E614–E621, 2003.
First published March 25, 2003; 10.1152/ajpendo.00267.2002.

Targeting of iNOS with antisense DNA plasmid reduces cytokine-induced inhibition of osteoblastic activity

Takahiro Abe,[1] Hisako Hikiji,[1,3] Wee Soo Shin,[2,3] Noboru Koshikiya,[1,3] Sei-ichi Shima,[1,3] Jumi Nakata,[1,3] Takafumi Susami,[1] Tsuyoshi Takato,[1] and Teruhiko Toyo-oka[2,3]

Departments of [1]Oral and Maxillofacial Surgery and [2]Organ Pathophysiology and Internal Medicine and [3]Health Service Centre, Faculty of Medicine, University of Tokyo, Tokyo 113-8655, Japan

Submitted 17 June 2002; accepted in final form 14 March 2003

Abe, Takahiro, Hisako Hikiji, Wee Soo Shin, Noboru Koshikiya, Sei-ichi Shima, Jumi Nakata, Takafumi Susami, Tsuyoshi Takato, and Teruhiko Toyo-oka. Targeting of iNOS with antisense DNA plasmid reduces cytokine-induced inhibition of osteoblastic activity. *Am J Physiol Endocrinol Metab* 285: E614–E621, 2003. First published March 25, 2003; 10.1152/ajpendo.00267.2002.—Proinflammatry cytokines, tumor necrosis factor-α combined with interleukin-1β, induce excessive production of nitric oxide (NO) and its cytotoxic metabolite peroxynitrite ($ONOO^-$) via inducible nitric oxide synthase (iNOS) in murine osteoblasts. In this study, to properly estimate the effects of antisense DNA of iNOS on osteoblastic activity, we produced transformed cell lines with antisense plasmid that specifically targets the iNOS gene for potential long-lasting inhibition. Transformed antisense cell lines were identified by *1*) the detection of antisense transcripts, *2*) the attenuated expression of iNOS protein, *3*) the reduction of NO synthase activity, and *4*) the level of NO production. These cell lines targeting iNOS, which showed decreased production of both NO and $ONOO^-$, prevented the inhibition of osteoblastic differentiation as was assayed by the mRNA expression of type I collagen, alkaline phosphatase, osteocalcin, and Core binding factor in the presence of proinflammatory cytokines. Present results indicate that the antisense DNA plasmid of iNOS is potent to reduce the cytokine-induced inhibition of osteoblastic activity.

inducible nitric oxide synthase; antisense; peroxynitrite; osteoblast

NITRIC OXIDE (NO) produced from L-arginine by NO synthase (NOS) has diverse functions in a variety of organs (34, 35). So far, three isoforms of the NOS have been isolated, *1*) endothelial (eNOS), 2) neuronal (nNOS), producing small quantities of NO in response to intracellular calcium ions, and 3) the inducible isoform (iNOS) expressed after exposure to bacterial endotoxin or inflammatory cytokines.

Tumor necrosis factor (TNF)-α and interleukin (IL)-1β enhance bone resorption (4, 27, 36, 39–41) and may lead to inflammatory diseases such as rheumatoid arthritis and osteoporosis under several pathological settings (13). These cytokines are reported to cause iNOS gene expression (21, 24) and actual NO production (10, 24, 36). In contrast, NO itself enhances osteoblastic differentiation in vitro (20). Therefore, these contradictory results suggest that the bone-resorbing effect of cytokines is not mediated via NO per se (20, 21, 41). NO reacts with superoxide (O_2^-) to form the highly reactive intermediate peroxynitrite ($ONOO^-$), a potent cytotoxic intermediate (26, 29, 44). $ONOO^-$, which is produced during an inflammatory response, causes a variety of toxic effects, including lipid peroxidation and tyrosine nitration on several biomolecules (22, 26). We showed previously that the cytokines actually generate both NO and O_2^- in osteoblasts and that NO and O_2^- produce an even more toxic product, $ONOO^-$, modifying osteoblastic differentiation (20). We have postulated that the cytokine-induced iNOS, not eNOS or nNOS, plays an important role in the inhibition of osteoblastic differentiation (20, 21).

The purpose of the present study is to examine effects of the specific inhibition of iNOS expression on osteoblastic cells and to inspect whether iNOS antisense plasmid prevents cytokine-induced reduction of osteoblastic activity. The biosynthesis of NO is competitively inhibited by several guanidine-substituted arginine analogs (5, 16). Although these chemical inhibitors of NOS are often used when inhibiting NOS and new-type inhibitors are being developed, they are not specific enough for each isoform of NOS and may have additional actions as analogs of essential amino acids (5, 33). In contrast, the antisense technique is specific for inhibiting the biosynthesis of a single protein. Further antisense plasmids have advantages over synthetic antisense oligonucleotides because oligonucleotides must be repeatedly added at high concentrations in culture medium and are not suitable for the long-term experiment (17). Antisense DNA plasmid, but not oligonucleotides, has the potential for long-lasting expression and thus may be used as a therapeutic approach to chronic disease. Here, we established stable transformants derived from osteoblastic MC3T3-E1 cells in which transfected plasmids continuously produced iNOS antisense RNA. With these cells, we investigated the specific effects of iNOS inhibition on alkaline phosphatase (ALPase) activity and levels of

Address for reprint requests and other correspondence: H. Hikiji, Dept. of Oral and Maxillofacial Surgery, Faculty of Medicine, Univ. of Tokyo, 7–3-1, Hongo, Bunkyo-ku 113–8655, Tokyo, Japan (E-mail: hikiji-ora@h.u-tokyo.ac.jp).

The costs of publication of this article were defrayed in part by the payment of page charges. The article must therefore be hereby marked "*advertisement*" in accordance with 18 U.S.C. Section 1734 solely to indicate this fact.

0193-1849/03 $5.00 Copyright © 2003 the American Physiological Society

American Journal of Physiology — Endocrinology and Metabolism

Downloaded from ajpendo.physiology.org on October 19, 2005

mRNA expression in type I collagen (COL I), ALPase, osteocalcin (OSC), and Core binding factor (Cbfa1), all of which are established indexes of osteoblastic differentiation (43).

MATERIALS AND METHODS

Cell culture. Murine osteoblastic MC3T3-E1 cells (RIKEN RCB1126) were cultured in α-MEM (GIBCO, Grand Island, NY) containing 10% FBS (JRH Bioscience, Lenexa, KS). The cells were incubated at 37°C in humidified air including 5% CO_2 and passaged every 7 days. The medium was changed every 2–3 days. Cellular confluence was maintained throughout all treatment procedures.

The responses to cytokine stimulation are variable among cells and tissues (10, 24). We found a combination of recombinant TNF-α (10 ng/ml; Dainippon Pharmaceutical, Tokyo, Japan) and IL-1β (10 ng/ml; Genzyme, Cambridge, MA) to be the sufficient concentration of these cytokines to stimulate the MC3T3-E1 cells (20).

Preparation of plasmids containing antisense or sense sequence of iNOS. Murine iNOS mRNA was isolated from MC3T3-E1 cells stimulated by cytokines and used to synthesize the first-strand cDNA with RT. cDNA was used as a template in a PCR with a primer (*primer 1*) designed from the sequence of murine macrophage iNOS (upper: 52–71 bp; lower: 264–245 bp; GenBank M84373; see Ref. 31). The 213-bp product, which covered the ATG initiation codon of the murine iNOS gene, was purified and subcloned into the plasmid vector pTARGET (Promega, Madison, WI) by blunt-end ligation.

After making large-scale preparation of the plasmids of interest by CsCl-ethidium bromide gradients, we performed three experiments to determine the orientation of the insert (antisense or sense direction with respect to the CMV promoter/enhancer). First, digestion with the restriction enzyme *Hinc* II (New England BioLabs, Beverly, MA) was carried out. Second, PCR was performed for the resultant plasmid with *primer 1* and *primer 2*, which were designed from the sequence of pTARGET. Finally, the insert was identified by direct sequencing of the PCR products.

Stable transfection of MC3T3-E1 cells. MC3T3-E1 cells were transfected using a lipofectamine reagent (GIBCO) according to the manufacturer's instruction. Briefly, the transfection was conducted for 4 h at 37°C in 5% CO_2 by adding 5 μg plasmid DNA (antisense, sense, and empty vector) to 20 μl of lipofectamine reagent in each well of six-well plates. At the end of 4 h of incubation, the culture medium was replaced with fresh 10% FBS containing α-MEM.

After 24 h, the medium was replaced with culture medium containing 0.5 mg/ml neomycin (G418; Wako Pure Chemical Industries, Osaka, Japan) to isolate stable transfectants in 10-cm dishes. After three more days, the medium was exchanged with fresh selection medium and then changed every 3 days thereafter until G418-resistant colonies appeared. Transfectants were selected as "positive" if they were resistant to 0.5 mg/ml G418. The lowest concentration of G418 used was that in which nontransfected MC3T3-E1 cells died within 10–14 days. Single colonies were isolated and expanded in culture. Transcription of the iNOS inserts in either the antisense or sense orientation was confirmed by RT-PCR with *primer 2* in each transfectant. NADPH diaphorase staining (see below), as a marker of NOS activity, immunocytochemistry of the iNOS protein, and the Griess reaction for NO production were added to confirm positive cell lines.

Immunocytochemistry of iNOS and nitrotyrosine. MC3T3-E1 cells on eight-well chamber slides (LAB-TEK II; Nalge Nunc International, Rochester, NY) were cultured for either 24 h for iNOS staining or 48 h for nitrotyrosine (NT) staining in the medium with or without cytokines. After being fixed in an ethanol-acetone mixture, the endogenous peroxidase was inactivated by 3% H_2O_2 in methanol.

Anti-iNOS polyclonal rabbit antibody (Santa Cruz Biotech, Santa Cruz, CA) or anti-NT polyclonal rabbit antibody (Upstate Biotech, Lake Placid, NY) was used as the first antibody, and rabbit IgG was used as the negative control. Cells were treated with the blocking reagent (Histofine; Nichirei, Tokyo, Japan) for 20 min and then with iNOS antibody for 3 h or NT antibody for 5 h at room temperature. These cells were then incubated with the secondary antibody (Simple stain MAX PO reagent; Nichirei), which consists of amino acid polymers conjugated to peroxidase and anti-mouse/rabbit IgG that is reduced to its F(ab)' fragment, at room temperature for 30 min. The immunoproduct was visualized by 3,3'-diaminobenzidine (Simple stain DAB reagent; Nichirei) according to the manufacturer's instructions and photographed by a digital camera (AX80; Olympus, Tokyo, Japan). The stained intensity was measured by densitometry with graphic software (version 6; Adobe Photoshop, Mountain View, CA). Precision of the intensity measurement was evaluated by making an arbitrary selection in the staining area and performing a double-blind test.

NADPH diaphorase staining. NOS has an activity of NADPH diaphorase that has been employed for histochemistry (12). Cells were grown to 100% confluence and incubated with or without cytokines for an additional 24 h. After cytokine stimulation, these cells were washed by PBS including 0.1% $CaCl_2$ [PBS(+)] and fixed in 2% formaldehyde. These cells were then washed three times and reacted in PBS(+) containing 1 mM β-NADPH and 0.2 mM nitroblue tetrazolium (Sigma, St. Louis, MO) for 30 min at 37°C.

Measurement of NO and ALPase activity. MC3T3-E1 cells were grown to 100% confluence and incubated with or without cytokines for a further 24 h. Nitrate and nitrite are stable after being formed from NO. Nitrate in the sample was converted to nitrite with nitrate reductase and then measured by spectrophotometry after the Griess reaction (19, 21).

The level of ALPase activity in bone tissues reflects osteoblastic differentiation (43). MC3T3-E1 cells were cultured on 24-well plates and stimulated by cytokines for 48 h. The ALPase activity (Wako) was assayed as described previously (21) and normalized by protein amount measured by the Bradford method (Bio-Rad Laboratories, Hercules, CA; see Ref. 21).

Cell proliferation assay. For measurement of cell proliferation, MC3T3-E1 cells and transfected cell lines were plated at a density of 4 × 10 cells/well on 96-well plates. After 24 h, medium was replaced with α-MEM containing 10% FBS in the absence or presence of cytokines and cultured for three more days. The effects of iNOS antisense on proliferation with or without cytokines were determined by a tetrazolium compound [3-(4,5-dimethylthiazol-2-yl)-5-(3-carboxymethoxyphenyl)-2-(4-sulfophenyl)-2H-tetrazolium, inner salt; MTS] assay (Promega). Briefly, 20 μl of MTS solution reagent were added to 100 μl of culture medium of each well. After incubation for 4 h at 37°C, the absorbance was measured at 490 nm using a 96-well plate reader (PowerWave ×340; Bio-Tek, Winooski, VT).

RT-PCR of COL I, ALPase, OSC, and Cbfa1 gene. The OSC message was detected by semiquantitative RT-PCR. MC3T3-E1 cells were cultured on 6-cm-diameter dishes and stimulated by the cytokines for 48 h. Total RNA was ex-

American Journal of Physiology — Endocrinology and Metabolism

Downloaded from ajpendo.physiology.org on October 19, 2005

tracted by ISOGEN (Nippon Gene, Toyama, Japan), and 2 μg of total RNA were reverse transcribed using Moloney murine leukemia virus RT (Superscript; GIBCO) for OSC, 1 μg total RNA was reverse transcribed using Avian myeloblastis virus RT (Roche, Indianapolis, IN) for COL I, ALPase, and Cbfa1, and the cDNA served for the following PCR template.

The PCR reaction was carried out as described previously (20, 21). cDNA was amplified by *Taq* DNA polymerase (Perkin-Elmer and Roche) using the following primers: OSC, 5′-GCCCTCTCCAAGACATATA-3′ and 5′-CCATGATCACGTCGATATCC-3′; COL I, 5′-ATGAGGACCCTCTCTCTGCT-3′ and 5′-CCGTAGATGCGTTTGTAGGC-3′; ALPase, 5′-GTGTGAATTGTTGGGGCTTT-3′ and 5′-ACCTGGGATGATTGAACTGG-3′; Cbfa1, 5′-TCTCTACTATGGTACTTCGT-3′ and 5′-AAGATCATGACTAGGGATTG-3′; and internal standard gene (GAPDH), 5′-TGAAGGTCGGTGTGAACGGATTTGGC-3′ and 5′-CATGTAGGCCATGAGGTCCACCAC-3′. The denaturing, annealing, and elongating conditions for the PCR reaction were 94, 50 or 57 or 60, and 72°C, respectively, with an initial 9-min denaturation and an additional 7-min extension step at 72°C. The PCR conditions were determined so that the band intensity showed a linear relationship with increases in the cycle number (26 cycles for OSC and ALPase, 30 cycles for COL I and Cbfa1). Bands were quantified by densitometry (Epi-Light UV FA500; Aisin Cosmos R&D, Tokyo, Japan), and the intensities were normalized with reference to GAPDH.

Statistics. All values are expressed as means ± SD. Statistical difference between values was examined by one-way ANOVA followed by Scheffé's multiple comparison test. P values <0.05 were considered to be statistically significant.

RESULTS

Stable gene expression of inserts. To ascertain whether the transformants express the transcripts of the inserts in a stable manner, RT-PCR was carried out using primers designed from the multiple cloning site of pTARGET vector. Without treatment of the cytokines, transcripts of the insert cDNA were detected constitutively, as bands, for either the antisense or sense RNA in transformed cells (Fig. 1), and they were not detected in the cell lines where an empty vector (pTARGET) was transfected. Bands were recognized in cell lines transfected with antisense or sense iNOS. These bands were detected in both sense and antisense orientations after three passages in a stable manner. Bands of GAPDH as an internal control were always recognized in all cells.

Immunodetection of iNOS. iNOS expression in MC3T3-E1 cells was investigated by immunocytochemistry (Fig. 2). iNOS was not detected in negative controls that employed unimmunized IgG or unstimulated cells (Fig. 2, *A*, *B*, *D*, *F*, and *H*). After stimulation by TNF-α and IL-1β, iNOS protein was recognized for wild-type cell lines in which vectors were not transfected (wild-type lines; Fig. 2*C*). For the cell lines in which an empty vector was transfected (vector control lines; Fig. 2*E*), and those in which a sense vector was transfected (sense lines; Fig. 2*G*), iNOS protein was also observed after cytokine stimulation. In contrast, for the cell lines in which iNOS antisense was transfected (antisense lines; Fig. 2*I*), iNOS protein was less detectable after cytokine stimulation. Densitometry of the staining revealed 14 ± 6, 13 ± 4, 12 ± 7, and 18 ± 6 in a wild-type cell line, a vector control line, a sense line, and an antisense line, respectively (Fig. 2, *B*, *D*, *F*, and *H*). After cytokine stimulation, the corresponding levels of staining intensity were 65 ± 8, 83 ± 12, 79 ± 18, and 18 ± 5 (Fig. 2, *C*, *E*, *G*, and *I*). These results

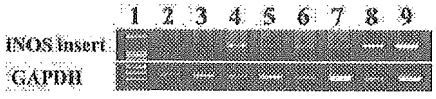

Fig. 1. Detection of antisense or sense inducible nitric oxide synthase (iNOS) mRNA using RT-PCR. Expression of the antisense or sense iNOS mRNA without the stimulation of tumor necrosis factor-α (TNF-α) and interleukin-1β (IL-1β) is shown. Cells were grown to 100% confluence without cytokine stimulation, and RT-PCR was carried out as described under MATERIALS AND METHODS. Expected product sizes for the inserts (antisense or sense) and GAPDH were 404 and 988 bp, respectively. DNA size marker (*lane 1*), wild-type cells (*lane 2*), vector control transfected with empty vector plasmid in MC3T3-E1 cells (vector control line, *lane 3*), cell lines in which sense vector was transfected (sense lines, *lanes 4–6*), and cell lines in which antisense vector was transfected (antisense lines, *lane 7–9*).

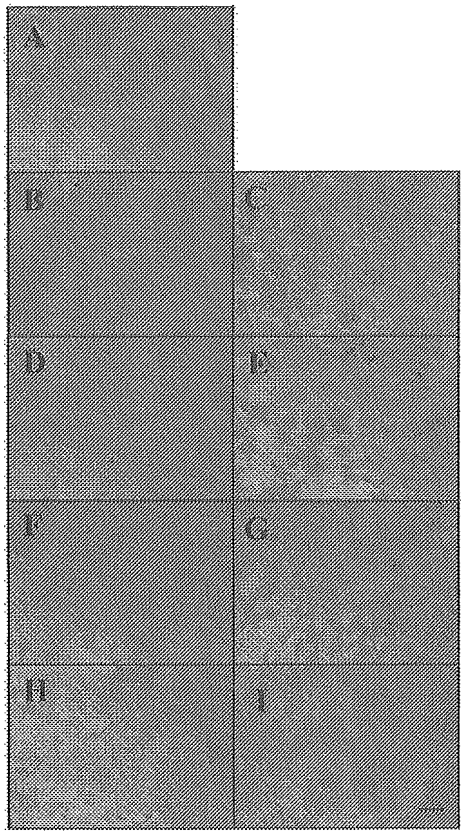

Fig. 2. Immunocytochemistry of iNOS after cytokine stimulation. Cells were grown to 100% confluence with TNF-α (10 ng/ml) and IL-1β (10 ng/ml) stimulation for 24 h. *A*: negative control in wild-type cells stained by control IgG; *B*: unstimulated wild-type cells; *C*: positive control in wild-type cells after cytokine stimulation; *D*: unstimulated, empty vector control line; *E*: empty vector control line after cytokine stimulation; *F*: unstimulated sense line; *G*: sense line after cytokine stimulation; *H*: unstimulated antisense line; *I*: antisense line after cytokine stimulation. Note that iNOS protein was selectively expressed in the cytoplasm and that the antisense line exhibits the production of iNOS after cytokine stimulation. Bar length, 100 μm.

American Journal of Physiology — Endocrinology and Metabolism

Downloaded from ajpendo.physiology.org on October 19, 2005